Inorg. Chem. **2002**, *41*, 5255–5268

Phosphine and Phosphonite Complexes of a Ruthenium(II) Porphyrin. 1. Synthesis, Structure, and Solution State Studies

Eugen Stulz,* Michael Maue, Neil Feeder, Simon J. Teat, Yiu-Fai Ng, Andrew D. Bond, Scott L. Darling, and Jeremy K. M. Sanders*

University Chemical Laboratory, University of Cambridge, Lensfield Road, Cambridge, CB2 1EW, U.K.

Received May 17, 2002

We have investigated the effect of complexation of different phosphorus ligands on the stability, solid state structure, and spectroscopic properties (NMR, IR, UV–vis) of a 5,15-diphenyl-substituted ruthenium porphyrin, (MeOH)Ru^{II}(CO)(DPP) **2** [DPP = 5,15-bis(3′,5′-di-*tert*-butyl)phenyl-2,8,12,18-tetraethyl-3,7,13,17-tetramethylporphyrin]. The ligands used are PPh_3, diphenyl(phenylacetenyl)phosphine (DPAP), bis(diphenylphosphino)acetylene (DPPA), tris(phenylacetenyl)phosphine [$(PA)_3P$], and diethyl (phenylacetenyl)phosphonite [$PAP(OEt)_2$]. The mono-phosphine complexes $(PR_3)Ru^{II}$(CO)(DPP) are readily formed in solution in quantitative yields. The complexes display association constants ranging from 1.2×10^4 M^{-1} for PPh_3 to 4.8×10^6 M^{-1} for $PAP(OEt)_2$. The weak association of PPh_3 does not correlate with its pK_a, $\delta(^{31}P)$, or cone angle value and is attributed to steric effects. Due to their kinetic lability, which is shown by 2D NMR spectroscopy, and the weakening of the carbonyl ligand via a trans effect, the mono-phosphine complexes could not be isolated. IR spectroscopy gives the relative order of π-acceptor strength as PPh_3 < DPAP, DPPA < $(PA)_3P$ < $PAP(OEt)_2$, whereas the relative order of the σ-donor strength is PPh_3 < $(PA)_3P$ < DPAP, DPPA < $PAP(OEt)_2$, based on the calculated pK_a values and on the $^{31}P\{^1H\}$ NMR chemical shifts of the ligands. The chemical shift differences in the $^{31}P\{^1H\}$ NMR spectra upon ligand binding display a linear correlation with the calculated pK_a values of the protonated ligands HPR_3^+; we propose that the pK_a, and probably other electronic properties, of a specific phosphorus ligand can be estimated on the basis of the chemical shift difference $\Delta\delta(^{31}P)$ upon complexation to a metalloporphyrin. The bis-phosphine complexes can be isolated in pure form by crystallization from $CHCl_3$–MeOH solutions using excess ligand. Association of the second ligand is in the same order of magnitude as the first binding for the phosphines, but the second phosphonite binding is decreased by a factor of about 100. The solid state structures show only marginal differences in the geometrical parameters. The calculated and the crystallographic cone angles of the ligands generally do not match, apart from the values obtained for $PAP(OEt)_2$.

Introduction

Multiporphyrinic arrays constructed through covalent or noncovalent connections have potential in acting as photochemical devices,[1,2] electronic multibit storage units,[3] or mimics of the natural photosynthetic system.[4] One promising approach is the self-assembly of heterometallic oligomers via orthogonal metal−ligand binding according to Pearson's HSAB principle.[5] The key to our strategy is to attach covalently a potential ligand onto a first metalloporphyrin, which is specifically chosen to recognize selectively a second metalloporphyrin with a different metal, thus preventing self-recognition. So far, we have made use of the known preferences of Zn(II), Ru(II), and Rh(III) for nitrogen and Sn(IV) for oxygen. In this way, we have been able to synthesize assemblies of heterometallic oligoporphyrins using cooperative zinc−nitrogen, ruthenium−nitrogen, and tin−oxygen coordination chemistry,[5] and recently an undecamer, containing porphyrins in four different metalation states.[6]

* To whom correspondence should be addressed. E-mail: es255@cam.ac.uk (E.S.); jkms@cam.ac.uk (J.K.M.S.).

(1) (a) Yamaguchi, H.; Kamachi, M.; Harada, A. *Angew. Chem., Int. Ed.* **2000**, *39*, 3829. (b) Norsten, T. B.; Branda, N. R. *J. Am. Chem. Soc.* **2001**, *123*, 1784. (c) Imahori, H.; Arimura, M.; Hanada, T.; Nishimura, Y.; Yamazaki, I.; Sakata, Y.; Fukuzumi, S. *J. Am. Chem. Soc.* **2001**, *123*, 335. (d) Cho, H. S.; Jeong, D. H.; Yoon, M. C.; Kim, Y. H.; Kim, Y. R.; Kim, D.; Jeoung, S. C.; Kim, S. K.; Aratani, N.; Shinmori, H.; Osuka, A. *J. Phys. Chem. A* **2001**, *105*, 4200. (e) Shediac, R.; Gray, M. H. B.; Uyeda, H. T.; Johnson, R. C.; Hupp, J. T.; Angiolillo, P. J.; Therien, M. J. *J. Am. Chem. Soc.* **2000**, *122*, 7017.

10.1021/ic025727y CCC: $22.00
Published on Web 09/12/2002

Chart 1

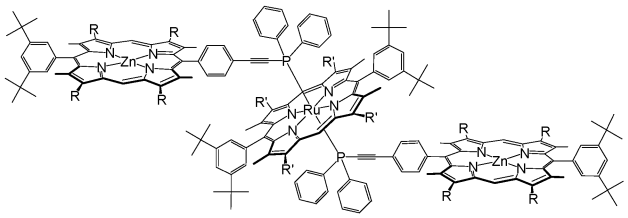

[**Zn/Ru/Zn**] **1**, R = hexyl, R' = ethyl

To expand our repertoire of orthogonal binding modes, we have become interested in the use of phosphorus as ligand for ruthenium porphyrins. We have shown that phosphine-substituted porphyrins are versatile building blocks for the construction of supramolecular assemblies,[7] including selection and virtually quantitative amplification of a thermodynamically stabilized, heterometallic, tetraporphyrinic construct from a dynamic combinatorial library.[8] In view of possible photophysical applications, the use of phosphorus to connect porphyrins via coordination chemistry to ruthenium(II), together with the immense diversity accessible by the variation of the substituents on the coordinating phosphorus, should offer a convenient means for fine-tuning the physical properties of assemblies. In order to predict electronic interactions in arrays such as the [Zn/Ru/Zn] trimer **1** (Chart 1),[7] it is advantageous to have detailed knowledge about the structure and physical properties of phosphorus metalloporphyrin complexes.

Trivalent phosphorus has been used as ligand for metalloporphyrins for several decades. Investigations have mainly been focused on ferrous,[9,10] ferric,[11−13] Co(II),[14] Ru(II),[15−18] and Rh(II)[19] porphyrins. Some phosphorus ruthenium(II) porphyrin complexes have been isolated and characterized, namely, Ru^{II}(TPP) (TPP = tetraphenylporphyrin) and Ru^{II}(OEP) (OEP = octaethylporphyrin) complexes of PPh_3,[15,16] of P(*p*-MeOPh)$_3$,[15] of PBu_3,[16,20] and of PF_3.[21] Cheng et al.[18] have described a (PBu_3)Ru^{II}(TPTBP) complex, the porphyrin being a structural hybrid of TPP and tetrabenzoporphyrin (TBP). To date no systematic study has been performed where different phosphorus ligands were complexed to a structurally fixed Ru(II) porphyrin.

Chart 2

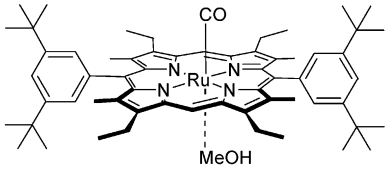

(MeOH)Ru^{II}(CO)(DPP) **2**

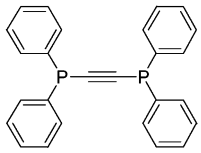

DPPA **3**

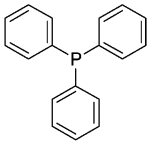

PPh_3 **4**

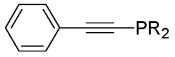

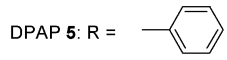

DPAP **5**: R =

PAP(OEt)$_2$ **6**: R =

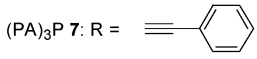

(PA)$_3$P **7**: R =

We now have investigated the effect of different phosphorus ligands on stability, solid state structure, and spectroscopic properties (NMR, IR, UV−vis) upon complexation to (MeOH)Ru^{II}(CO)(DPP) **2** [DPP = 5,15-bis(3′,5′-di-*tert*-butyl)phenyl-2,8,12,18-tetraethyl-3,7,13,17-tetramethylporphyrin, Chart 2]. Photophysical and electrochemical studies as well as EHMO calculations on these model complexes will be described in the following paper.[61] In our series of phosphorus ligands, one phenylalkynyl substituent was held constant [except for bis(diphenylphosphino)acetylene, DPPA **3**] matching the substitution pattern of our phosphorus-

(2) Mak, C. C.; Bampos, N.; Darling, S. L.; Montalti, M.; Prodi, L.; Sanders, J. K. M. *J. Org. Chem.* **2001**, *66*, 4476.
(3) (a) Gryko, D. T.; Clausen, C.; Roth, K. M.; Dontha, N.; Bocian, D. F.; Kuhr, W. G.; Lindsey, J. S. *J. Org. Chem.* **2000**, *65*, 7345. (b) Li, J. Z.; Gryko, D.; Dabke, R. B.; Diers, J. R.; Bocian, D. F.; Kuhr, W. G.; Lindsey, J. S. *J. Org. Chem.* **2000**, *65*, 7379. (c) Collman, J. P.; Kendall, J. L.; Chen, J. L.; Collins, K. A.; Marchon, J. C. *Inorg. Chem.* **2000**, *39*, 1661.
(4) (a) Haycock, R. A.; Hunter, C. A.; James, D. A.; Michelsen, U.; Sutton, L. R. *Org. Lett.* **2000**, *2*, 2435. (b) Gust, D.; Moore, T. A.; Moore, A. L. *Acc. Chem. Res.* **2001**, *34*, 40. (c) Imahori, H.; Norieda, H.; Yamada, H.; Nishimura, Y.; Yamazaki, I.; Sakata, Y.; Fukuzumi, S. *J. Am. Chem. Soc.* **2001**, *123*, 100. (d) Sun, L.; Hammarstrom, L.; Akermark, B.; Styring, S. *Chem. Soc. Rev.* **2001**, *30*, 36.
(5) Kim, H. J.; Bampos, N.; Sanders, J. K. M. *J. Am. Chem. Soc.* **1999**, *121*, 8120.
(6) Redman, J. E.; Feeder, N.; Teat, S. J.; Sanders, J. K. M. *Inorg. Chem.* **2001**, *40*, 2486.
(7) Darling, S. L.; Stulz, E.; Feeder, N.; Bampos, N.; Sanders, J. K. M. *New J. Chem.* **2000**, *24*, 261.
(8) Stulz, E.; Ng, Y.-F.; Scott, S. M.; Sanders, J. K. M. *Chem. Commun.* **2002**, 524.
(9) (a) Simonneaux, G.; Sodano, P. *Inorg. Chem.* **1988**, *27*, 3956. (b) Simonneaux, G.; Sodano, P. *J. Organomet. Chem.* **1988**, *349*, C11. (c) Guillemot, M.; Simonneaux, G. *J. Chem. Soc., Chem. Commun.* **1995**, 2093.
(10) Pilard, M. A.; Guillemot, M.; Toupet, L.; Jordanov, J.; Simonneaux, G. *Inorg. Chem.* **1997**, *36*, 6307.
(11) Sodano, P.; Simonneaux, G.; Toupet, L. *J. Chem. Soc., Dalton Trans.* **1988**, 2615.
(12) (a) Rieger, P. H. *Coord. Chem. Rev.* **1994**, *135*, 203. (b) Ohya, T.; Morohoshi, H.; Sato, M. *J. Pharmacobio-Dyn.* **1985**, *8*, S14.
(13) Ohya, T.; Morohoshi, H.; Sato, M. *Inorg. Chem.* **1984**, *23*, 1303.
(14) Wayland, B. B.; Sherry, A. E.; Bunn, A. G. *J. Am. Chem. Soc.* **1993**, *115*, 7675.
(15) Ariel, S.; Dolphin, D.; Domazetis, G.; James, B. R.; Leung, T. W.; Rettig, S. J.; Trotter, J.; Williams, G. M. *Can. J. Chem.* **1984**, *62*, 755.
(16) Chow, B. C.; Cohen, I. A. *Bioinorg. Chem.* **1971**, *1*, 57.
(17) James, B. R.; Dolphin, D.; Leung, T. W.; Einstein, F. W. B.; Willis, A. C. *Can. J. Chem.* **1984**, *62*, 1238.
(18) Cheng, R. J.; Lin, S. H.; Mo, H. M. *Organometallics* **1997**, *16*, 2121.
(19) (a) Grass, V.; Lexa, D.; Momenteau, M.; Saveant, J. M. *J. Am. Chem. Soc.* **1997**, *119*, 3536. (b) Collman, J. P.; Boulatov, R. *J. Am. Chem. Soc.* **2000**, *122*, 11812.
(20) (a) Tsutsui, M.; Osterfeld, D.; Hoffman, L. M. *J. Am. Chem. Soc.* **1971**, *93*, 1820. (b) Tsutsui, M.; Osterfeld, D.; Francis, J. N.; Hoffman, L. M. *J. Coord. Chem.* **1971**, 115. (c) Barley, M.; Becker, J. Y.; Domazetis, G.; Dolphin, D.; James, B. R. *Can. J. Chem.* **1983**, *61*, 2389.
(21) Kadish, K. M.; Hu, Y.; Tagliatesta, P.; Boschi, T. *J. Chem. Soc., Dalton Trans.* **1993**, 1167.

substituted porphyrins, as shown in **1**, to enable direct comparisons to be made. This should allow direct application of the results obtained from this study to porphyrin-substituted phosphines in supramolecular structures. PPh_3 **4** was added to the series for comparison with known literature data for TPP and OEP.[15,16]

Generally, the physicochemical properties of phosphorus complexes are influenced by both steric and electronic effects. Steric effects are most commonly expressed in terms of Tolman's cone angle θ,[22] obtainable from crystallographic data.[23] Electronic effects are controlled by a combination of σ-donor and π-acceptor properties. σ-Donation usually decreases in the order phosphine > phosphonite, e.g., in going from diphenyl(phenylacetenyl)phosphine (DPAP **5**) to diethyl (phenylacetenyl)phosphonite [PAP(OEt)$_2$ **6**].[13] π-Acidity, on the other hand, is expected to be increased for phosphonites[10,24,25] compared to phosphines due to P(3d)−O(2pπ/2pπ*) orbital interactions. Substituting phenyl for alkyne, as in tris(phenylacetenyl)phosphine [(PA)$_3$P **7**], has an influence on both σ-donor[26] and π-acceptor[27] properties, and an increased electronic interaction between the phosphorus and the three acetylene substituents compared to **5** may be expected.[28] The same interactions should also lead to differences in the properties of the bis(diphenylphosphino)acetylene (DPPA **3**), where the acetylene unit bears two phosphorus atoms compared to DPAP. Overall, the ligands in our series were chosen to cover a wide range of substitution patterns and of electronic properties.

Experimental Section

All manipulations were performed using standard inert atmosphere techniques and freshly distilled and degassed solvents: methylene chloride (CH_2Cl_2), chloroform ($CHCl_3$), and tetrahydrofuran (THF) from CaH, and methanol (MeOH) from Mg; $CDCl_3$ was filtered over basic alumina and degassed by purging with Ar prior to use. (MeOH)Ru^{II}(CO)(DPP) (**2**),[2,29] DPAP (**5**),[30] and (PA)$_3$P (**7**)[31] were prepared using literature procedures. DPPA (**3**) was purchased from Strem Chemicals, and phenylacetylene, EtMgBr (1.0 M THF), and ClP(OEt)$_2$ were purchased from Aldrich (reagent grade). All chemicals were used as obtained.

NMR spectra were recorded on a Bruker DPX400 NMR spectrometer at 400.13 MHz (^{1}H, solvent as internal standard) or 161.98 MHz (^{31}P{^{1}H}, H_3PO_4 external standard), or on a Bruker DRX500 NMR spectrometer at 500.13 MHz (^{1}H) or 125.70 MHz (^{13}C, solvent as internal standard). Abbreviations for ^{1}H NMR spectra used are as follows: s, singlet; d, doublet; t, triplet; dt, doublet of triplets; m, multiplet; b, broad. UV−vis spectra were recorded on a Varian Cary 100 Bio spectrophotometer. IR spectra were obtained on a Perkin-Elmer Paragon 1000 FTIR spectrometer using CH_2Cl_2 as solvent (NaCl cell, 0.5 mm). The positive ESI-HRMS spectrum of **6** was recorded on a Micromass Q-TOF1 MS instrument.

X-ray diffraction data were collected for (DPAP)$_2$Ru^{II}(DPP) (triclinic form) and [PAP(OEt$_2$)]$_2$Ru^{II}(DPP) using a Nonius Kappa CCD diffractometer. Crystals of [(PA)$_3$P]$_2$Ru^{II}(DPP), (DPPA)$_2$-Ru^{II}(DPP), and (DPAP)$_2$Ru^{II}(DPP) (monoclinic form) were small and weakly diffracting, and data were collected for these at Station 9.8, Daresbury SRS, U.K., using a Bruker SMART CCD diffractometer. Structures were solved by direct methods using either SHELXS-97[32] or SIR-92[33] and refined against all F^2 data using SHELXL-97.[32] A summary of the crystallographic data is given in Table 1.

PAP(OEt)$_2$ (6).[34] Phenylacetylene (2.00 g, 19.6 mmol) was dissolved in THF (20 mL), and, after cooling to −78 °C (dry ice/acetone bath), a 1 M EtMgBr solution (19.6 mL) was slowly added via syringe. After 15 min of stirring at −78 °C, ClP(OEt)$_2$ (3.07 g, 19.6 mmol) in THF (10 mL) was added dropwise. The yellowish mixture was stirred for 30 min at −78 °C and warmed to room temperature, and the reaction was quenched by addition of 20 mL of saturated Na_2CO_3 aqueous solution. The mixture was poured into 1:1 CH_2Cl_2/H_2O (400 mL, purged with N_2). The organic phase was separated, washed once with H_2O (100 mL, N_2), dried ($MgSO_4$), and evaporated in vacuo. Column chromatography (silica, 5:1 hexane/EtOAc, N_2) gave **6** as a colorless oil. Yield: 3.68 g (16.6 mmol, 84%). The product is air sensitive and smelly; it should be stored under an inert atmosphere at −20 °C. ^{1}H NMR (400 MHz, $CDCl_3$): δ 7.48 (t, 2 H, *o-H*), 7.32 (m, 3 H, *m*/*p-H*), 4.04 (q, J = 6 Hz, 4 H, OCH_2CH$_3$), 1.31 (t, J = 6 Hz, 6 H, OCH$_2$CH_3) ppm. ^{13}C NMR (125.70 MHz, $CDCl_3$): δ 132.1, 129.3, 128.3, 121.6, 103.7 (d, $^2J_{P-C}$ = 3.4 Hz, P−C), 89.2 (d, $^1J_{P-C}$ = 42.6 Hz), 63.5 (d, $^2J_{P-C}$ = 6.8 Hz), 17.0 ppm. ^{31}P{^{1}H} NMR (162 MHz, $CDCl_3$): δ 131 ppm. ESI-HRMS: calcd for $C_{12}H_{16}O_2P$ [M + H$^+$] 223.0888, found 223.0881 [M + H$^+$].

Syntheses of the Mono-Phosphino Complexes (PR$_3$)Ru^{II}(CO)-(DPP). General Procedure. 2 (5.0 mg, 4.93 μmol) was suspended in 0.5 mL of solvent ($CDCl_3$ or CD_2Cl_2 for NMR studies, CH_2Cl_2 for UV−vis and IR measurement). Phosphine (10 equiv) was dissolved in 1.0 mL of solvent, and 100 μL was added via syringe to the porphyrin suspension. The solution was stirred at room temperature under Ar atmosphere until all starting material had dissolved (usually 15−30 min), and the orange solution was directly used for spectroscopic studies.

(DPAP)Ru^{II}(CO)(DPP) (8). IR (CH_2Cl_2): 1943 ($\nu_{C\equiv O}$) cm^{-1}. UV−vis (CH_2Cl_2): λ (log ϵ) 413 (5.12), 533 (4.08), 560 (3.52) nm. ^{1}H NMR ($CDCl_3$, 400 MHz): δ 9.72 (s, 2 H, por-meso*H*; por = porphyrinic), 7.82 (bs, 2 H, por-Ar*H*), 7.70 (bs, 2 H, por-Ar*H*), 7.33 (bs, 2 H, por-Ar*H*), 7.23 (m, 2 H, C≡CAr*H*), 7.21 (m, 2 H, C≡CAr*H*), 7.00 (dd, J = 6, 2 Hz, 4 H, C≡CAr*H*), 6.78 (dt, J = 7, 1 Hz, 4 H, PAr-p*H*), 6.47 (dt, J = 9, 2 Hz, 4 H, PAr-m*H*), 4.42 (m, 4 H, PAr-o*H*), 3.83 (q, J = 7 Hz, 8 H, por-CH_2CH$_3$), 1.57 (t, J = 7 Hz, 12 H, por-CH$_2$CH_3), 2.21 (bs, 12 H, por-CH_3), 1.48 (s, 36 H, Ar-^{t}Bu*H*) ppm. ^{31}P{^{1}H} NMR (162 MHz, $CDCl_3$): δ −13 ppm.

(DPPA)Ru^{II}(CO)(DPP) (9). IR (CH_2Cl_2): 1943 ($\nu_{C\equiv O}$) cm^{-1}. UV−vis (CH_2Cl_2): λ (log ϵ) 413 (5.09), 533 (4.04), 562 (3.27)

(22) Tolman, C. A. *Chem. Rev.* **1977**, *77*, 313.
(23) Müller, T. E.; Mingos, D. M. P. *Transition Met. Chem.* **1995**, *20*, 533.
(24) Fernandez, A. L.; Reyes, C.; Prock, A.; Giering, W. P. *J. Chem. Soc., Perkin Trans. 2* **2000**, *5*, 1033.
(25) Mathew, N.; Jagirdar, B. R. *Organometallics* **2000**, *19*, 4506.
(26) (a) Taft, R. W. *Steric Effects in Organic Chemistry*; John Wiley & Sons: New York, 1956. (b) Taft, R. W. *J. Am. Chem. Soc.* **1952**, *74*, 3120.
(27) Hengefeld, A.; Kopf, J.; Rehder, D. *Organometallics* **1983**, *2*, 114.
(28) Carty, A. J.; Hota, N. K.; Ng, T. W.; Patel, H. A.; O'Connor, T. J. *Can. J. Chem.* **1971**, *49*, 2706.
(29) Twyman, L. J.; Sanders, J. K. M. *Tetrahedron Lett.* **1999**, *40*, 6681.
(30) Carty, A. J.; Hota, N. K.; Ng, T. W.; Patel, H. A.; O'Connor, T. J. *Can. J. Chem.* **1971**, *49*, 2706.
(31) Bharathi, P.; Periasamy, M. *Organometallics* **2000**, *19*, 5511. Lang, H.; Zsolnai, L. *J. Organomet. Chem.* **1989**, *369*, 131.
(32) Sheldrick, G. M. *SHELXS-97*; University of Göttingen: Göttingen, Germany, 1997.
(33) Altomare, A.; Cascarano, G.; Giacovazzo, C.; Guagliardi, A.; Burla, M. C.; Polidori, G.; Camalli, M. *J. Appl. Crystallogr.* **1994**, *27*, 435.
(34) Gil, J. M.; Sung, J. W.; Park, C. P.; Oh, D. Y. *Synth. Commun.* **1997**, *27*, 3171.

Table 1. Crystallographic Data for $(DPAP)_2Ru(DPP)$ (**12**), Triclinic and Monoclinic Form, $[(PA)_3P]_2Ru(DPP)$ (**14**), and $[PAP(OEt)_2]_2Ru(DPP)$ (**15**)

	$(DPAP)_2Ru(DPP)$ (**12**)			
	triclinic	monoclinic	$[(PA)_3P]_2Ru(DPP)\cdot 4CHCl_3$ (**14**)	$[PAP(OEt)_2]_2Ru(DPP)$ (**15**)
formula	$C_{100}H_{106}N_4P_2Ru$	$C_{100}H_{106}N_4P_2Ru$	$C_{112}H_{110}Cl_{12}N_4P_2Ru$	$C_{84}H_{106}N_4O_4P_2Ru$
M	1526.90	1526.90	2100.45	1398.74
T/K	180(2)	150(2)	150(2)	180(2)
radiation, λ/Å	Mo Kα, 0.707	synchrotron, 0.6929	synchrotron, 0.6923	Mo Kα, 0.707
cryst size/mm	0.18 × 0.18 × 0.09	0.06 × 0.04 × 0.02	0.08 × 0.08 × 0.06	0.30 × 0.23 × 0.18
cryst syst	triclinic	monoclinic	triclinic	triclinic
space group	$P\bar{1}$	$C2/c$	$P\bar{1}$	$P\bar{1}$
a/Å	11.1136(5)	22.920(5)	13.8041(7)	9.8043(2)
b/Å	12.4931(5)	20.254(5)	13.8388(8)	10.7826(3)
c/Å	16.7167(7)	18.366(5)	14.7719(8)	18.6293(6)
α/deg	71.554(2)	90	87.730(2)	87.309(2)
β/deg	73.964(2)	102.44(1)	83.010(2)	77.381(2)
γ/deg	73.214(2)	90	67.105(2)	84.103(2)
V/Å^3	2063.8(2)	8326(4)	2580.2(2)	1911.1(1)
Z	1	4	1	1
ρ_{calcd}/g cm^{-3}	1.299	1.218	1.352	1.215
μ/mm^{-1}	0.279	0.276	0.544	0.298
θ_{max}/deg	25.0	20.3	29.4	27.5
total data	11339	13361	25065	21731
indep data	7184	4335	13243	8637
R_{int}	0.032	0.207	0.026	0.061
R1 [$F^2 > 2\sigma(F^2)$]	0.055	0.204	0.051	0.054
wR2 (all data)	0.136	0.506	0.137	0.149
S	1.20	1.82	1.04	1.04

nm. ^{1}H NMR ($CDCl_3$, 400 MHz): δ 9.97 (s, 2 H, por-meso*H*), 7.81 (bs, 2 H, por-Ar*H*), 7.70 (bs, 2 H, por-Ar*H*), 7.58 (bs, 2 H, por-Ar*H*), 7.17 (bs, 2 H, C≡CPAr*H*), 7.09 (m, 4 H, C≡CPAr*H*), 6.94 (m, 4 H, C≡CPAr*H*), 6.76 (bs, 2 H, Ru-PAr-p*H*), 6.39 (bs, 4 H, Ru-PAr-m*H*), 4.12 (bs, 4 H, PAr-o*H*), 3.80 (m, 8 H, por-CH_2-CH$_3$), 2.20 (bs, 12 H, por-CH_3), 1.76 (t, J = 7.1 Hz, 12 H, por-CH$_2$CH_3), 1.50 (s, 18 H, Ar-^{t}Bu*H*), 1.47 (s, 18 H, Ar-^{t}Bu*H*) ppm. ^{31}P{^{1}H} NMR (162 MHz, $CDCl_3$): δ −12 (Ru-*P*C≡C), −32 (C≡*P*Ph$_2$) ppm.

[(PA)$_3$P]Ru^{II}(CO)(DPP) (10). IR (CH_2Cl_2): 1955 ($\nu_{C\equiv O}$) cm^{-1}. UV−vis (CH_2Cl_2): λ (log ϵ) 412 (4.99), 532 (4.03), 560 (3.52) nm. ^{1}H NMR (CD_2Cl_2, 400 MHz): δ 10.10 (bs, 2 H, por-meso*H*), 7.99 (s, 2 H, por-Ar*H*), 7.90 (s, 2 H, por-Ar*H*), 7.85 (s, 2 H, por-Ar*H*), 7.27 (m, 3 H, C≡CAr*H*), 7.20 (m, 6 H, C≡CAr*H*), 6.96 (d, J = 8 Hz, 6 H, C≡CAr*H*), 3.73 (bs, 8 H, por-CH_2CH$_3$), 2.53 (bs, 12 H, por-CH_3), 1.85 (t, J = 8 Hz, 12 H, por-CH$_2$CH_3), 1.56 (s, 36 H, Ar-^{t}Bu*H*) ppm. ^{31}P{^{1}H} NMR (162 MHz, CD_2Cl_2): δ −59 ppm.

[PAP(OEt)$_2$]Ru^{II}(CO)(DPP) (11). IR (CH_2Cl_2): 1958 ($\nu_{C\equiv O}$) cm^{-1}. UV−vis (CH_2Cl_2): λ (log ϵ) 412 (5.01), 532 (3.97), 561 (3.22) nm. ^{1}H NMR ($CDCl_3$, 400 MHz): δ 9.74 (s, 2 H, por-meso*H*), 7.99 (s, 2 H, por-Ar*H*), 7.74 (s, 2 H, por-Ar*H*), 7.70 (s, 2 H, por-Ar*H*), 7.16 (t, J = 8 Hz, 2 H, C≡CAr*H*), 7.24 (m, 2 H, C≡CAr*H*), 6.80 (d, J = 7 Hz, 2 H, C≡CAr*H*), 3.80 (m, 8 H, por-CH_2CH$_3$), 2.16 (s, 12 H, por-CH_3), 1.67 (t, J = 8 Hz, 12 H, por-CH$_2$CH_3), 1.51 (s, 18 H, Ar-^{t}Bu*H*) ppm, 1.41 (s, 18 H, Ar-^{t}Bu*H*), 0.92/0.78 (m, 2 × 2 H, PO-CH_2CH$_3$), −0.18 (t, J = 7 Hz, PO-CH$_2$CH_3). ^{31}P{^{1}H} NMR (162 MHz, $CDCl_3$): δ 108 ppm.

Synthesis of Bis-Phosphino Complexes (PR$_3$)$_2$Ru^{II}(DPP). General Procedure. 2 (50 mg, 49.3 μmol) was suspended in $CHCl_3$ (5 mL), and neat phosphine (5 equiv) was added. The solution was stirred at room temperature under Ar atmosphere for 15 min, and the solvent was removed on a rotary evaporator. The residue was redissolved in 5 mL of $CHCl_3$ and stirred at room temperature for 10 min., and the solvent was removed in vacuo. The orange solid was dissolved in a minimum amount of hot $CHCl_3$ (ca. 2 mL), and 10 mL of MeOH was carefully layered over the solution. After standing overnight, orange to bronze colored crystals were collected on a sintered funnel, washed with MeOH, and dried in vacuo. Yields are in the range 90−98%.

(DPAP)$_2$Ru^{II}(DPP) (12). UV−vis (CH_2Cl_2): λ (log ϵ) 423 (5.44) nm. ^{1}H NMR ($CDCl_3$, 400 MHz): δ 9.13 (s, 2 H, por-meso*H*), 7.55 (s, 2 H, por-Ar*H*), 7.41 (s, 4 H, por-Ar*H*), 7.24 (m, 4 H, C≡CAr*H*), 7.18 (t, J = 7 Hz, 4 H, C≡CAr*H*), 6.95 (d, J = 7 Hz, 4 H, C≡CAr*H*), 6.69 (t, J = 8 Hz, 4 H, PAr-p*H*), 6.39 (t, J = 8 Hz, 8 H, PAr-m*H*), 4.38 (m, 8 H, PAr-o*H*), 3.45 (q, J = 7 Hz, 8 H, por-CH_2CH$_3$), 2.13 (s, 12 H, por-CH_3), 1.54 (t, J = 7 Hz, 12 H, por-CH$_2$CH_3), 1.41 (s, 36 H, Ar-^{t}Bu*H*). ^{31}P{^{1}H} NMR (162 MHz, $CDCl_3$): δ 3 ppm.

(DPPA)$_2$Ru^{II}(DPP) (13). UV−vis (CH_2Cl_2): λ (log ϵ) 423 (5.25) nm. ^{1}H NMR ($CDCl_3$, 500 MHz): δ 9.54 (s, 2 H, por-meso*H*), 7.55 (t, J = 2 Hz, 2 H, por-Ar*H*), 7.14 (d, J = 2 Hz, 4 H, por-Ar*H*), 7.08 (t, J = 9 Hz, 2 H, C≡CPAr-p*H*), 7.02 (dt, J = 9, 1 Hz, 4 H, C≡CPAr-m*H*), 6.93 (dt, J = 9, 1 Hz, 4 H, C≡CPAr-o*H*), 6.69 (t, J = 9 Hz, 4 H, Ru-PAr-p*H*), 6.32 (t, J = 9 Hz, 8 H, Ru-PAr-m*H*), 4.31 (m, 8 H, Ru-PAr-o*H*), 3.54 (q, J = 9 Hz, 8 H, por-CH_2CH$_3$), 1.94 (s, 12 H, por-CH_3), 1.65 (t, J = 9 Hz, 12 H, por-CH$_2$CH_3), 1.42 (s, 36 H, Ar-^{t}Bu*H*). ^{13}C NMR (125.70 MHz, $CDCl_3$): δ 148.1, 144.5, 143.0, 140.9, 140.3, 137.2, 135.6, 135.5, 138.1, 131.9, 129.2, 128.3, 128.1, 128.0, 127.0, 125.8, 119.7, 119.4, 104.3, 100.0, 35.4, 32.2, 20.1, 18.4, 15.0. ^{31}P{^{1}H} NMR (162 MHz, $CDCl_3$): δ 3 (Ru-*P*C≡CPPh$_2$), −30 ((Ru-PC≡C*P*Ph$_2$) ppm.

[(PA)$_3$P]$_2$Ru^{II}(DPP) (14). UV−vis (CH_2Cl_2): λ (log ϵ) 418 (5.37) nm. ^{1}H NMR (CD_2Cl_2, 500 MHz): δ 9.53 (s, 2 H, por-meso*H*), 7.60 (s, 4 H, por-Ar*H*), 7.58 (s, 2 H, por-Ar*H*), 7.16 (t, J = 7 Hz, 2 H, C≡CAr-p*H*), 7.10 (t, J = 8 Hz, 4 H, C≡CAr-m*H*), 6.89 (d, J = 7 Hz, 4 H, C≡CAr-o*H*), 3.52 (q, J = 7 Hz, 8 H, por-CH_2CH$_3$), 2.24 (s, 12 H, por-CH_3), 1.44 (t, J = 7 Hz, 12 H, por-CH$_2$CH_3), 1.17 (s, 36 H, Ar-^{t}Bu*H*). ^{13}C NMR (125.70 MHz, $CDCl_3$): δ 148.9, 144.7, 143.2, 141.2, 140.3, 140.0, 137.3, 137.2, 131.8, 128.9, 127.8, 120.9, 120.7, 100.8, 98.6, 34.5, 31.1, 19.8, 16.9, 15.0. ^{31}P{^{1}H} NMR (162 MHz, $CDCl_3$): δ −50 ppm. This complex is soluble in CH_2Cl_2, but not in $CHCl_3$.

[PAP(OEt)$_2$]$_2$Ru^{II}(DPP) (15). UV−vis (CH_2Cl_2): λ (log ϵ) 419 (5.64) nm. ^{1}H NMR ($CDCl_3$, 400 MHz): δ 9.33 (bs, 2 H, por-meso*H*), 7.75 (s, 4 H, por-Ar*H*), 7.66 (s, 2 H, por-Ar*H*), 7.20 (t, J = 7 Hz, 2 H, C≡CAr-p*H*), 7.12 (t, J = 7 Hz, 4 H, C≡CAr-m*H*), 6.83 (d, J = 7 Hz, 4 H, C≡CAr-o*H*), 3.63 (q, J = 7 Hz, 8 H, por-CH_2CH$_3$), 2.23 (s, 12 H, por-CH_3), 1.55 (t, J = 7 Hz, 12 H,

Chart 3

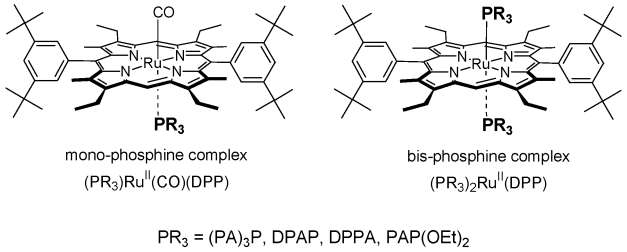

por-CH_2CH_3), 1.40 (s, 36 H, Ar-^{t}Bu*H*), 0.96 (t, J = 7 Hz, 2 H, PO-CH_2CH_3), 0.84 (t, J = 7 Hz, 2 H, PO-CH_2CH_3), −0.18 (t, J = 7 Hz, PO-CH_2CH_3). ^{13}C NMR (125.70 MHz, $CDCl_3$): δ 148.7, 144.2, 144.0, 143.2, 140.7, 139.9, 136.5, 131.7, 131.6, 128.4, 127.6, 121.4, 121.1, 119.9, 98.5 (d), 58.4, 34.8, 31.5, 19.6, 17.7, 15.1, 14.4. ^{31}P{^{1}H} NMR (162 MHz, $CDCl_3$): δ 114 ppm.

UV−Vis Titration of (L)Ru^{II}(CO)(DPP). The following stock solutions were prepared in degassed methylene chloride: **2**, 10^{-4} M; phosphine, 1.5 mM. The titrations were performed in a 0.1 mm quarz cuvette, using 300 μL of porphyrin solution. The phosphine was added in 2 μL aliquots (0.1 equiv) using a gastight syringe, until 1.5 equiv were added. The absorbance was measured in the range 350−650 nm after 2 min of equilibration. The association constants were determined using the changes in the molar extinction coefficient at 400, 411, 520, 534, and 551 nm; K_A and x_{SL} were determined by a least-squares fitting of the data according to eq 1,[35]

$$x_{obsd} = x_S + 0.5(x_{SL} - x_S)([S]_t + [L]_t + K_D - \{([S]_t + [L]_t + K_D)^2\} - 4[S]_t[L]_t)^{1/2})/[S]_t \quad (1)$$

where x = molar extinction coefficient (x_{obsd} = Abs/[S]), S = **2**, SL = mono-phosphine complex, $[X]_t$ = total concentration, and K_D = dissociation constant. For the calculations of x_{obsd}, an appropriate dilution factor was taken into account.

UV−Vis Titration of (L)$_2$Ru^{II}(DPP). The bis-phosphine complexes were prepared as 1 mM stock solutions in oxygen-free methylene chloride. Using a 0.1 mm quartz cuvette, 12 μL of the stock solution was added in 2 μL aliquots to 300 μL of methylene chloride, and the absorption spectra were measured after each addition (2 min of equilibration). The compositions of the mixtures were evaluated using baseline correction and peak deconvolution (Gaussian peak function) at ∼400, ∼411, and ∼423 nm, according to the complex measured. Using the known total concentration, and the extinction coefficients for **2** and the mono-phosphine complexes, the distribution was calculated at each concentration according to equilibria 2 and 3, using [**2**] = 0.5[phosphine]. The determined dissociation constants are an average of all individual concentrations.

$$Ru^{II}(DPP) + PR_3 \rightleftarrows (PR_3)Ru^{II}(DPP) \quad (2)$$

$$(PR_3)Ru^{II}(DPP) + PR_3 \rightleftarrows (PR_3)_2Ru^{II}(DPP) \quad (3)$$

Results

Synthesis and NMR Spectroscopy of Mono-Phosphine Complexes. The mono-phosphine complexes (DPAP)Ru^{II}(CO)(DPP), (DPPA)Ru^{II}(CO)(DPP), [(PA)$_3$P]Ru^{II}(CO)(DPP), and [PAP(OEt)$_2$]Ru^{II}(CO)(DPP) are readily synthesized in solution, simply by mixing equimolar amounts of phosphine and (MeOH)Ru^{II}(CO)(DPP) (Chart 3). All compounds are soluble in chloroform up to 10 mM concentrations, except for [(PA)$_3$P]Ru^{II}(CO)(DPP). This complex precipitated immediately after addition of **7** to (MeOH)Ru^{II}(CO)(DPP) in $CHCl_3$, but a freshly prepared sample retained its solubility in CH_2Cl_2. The ^{1}H NMR spectra showed the expected 1:1 ratio of the ligand to (MeOH)Ru^{II}(CO)(DPP). Figure 1 displays the ^{1}H NMR spectra of PAP(OEt)$_2$, [PAP(OEt)$_2$]-Ru^{II}(CO)(DPP), and [PAP(OEt$_2$)]$_2$Ru^{II}(DPP) as representative examples. Characteristic upfield shifts of the phosphorus phenyl substituents [$\Delta\delta$ = −0.4 ppm (*p*-H), −0.8 ppm (*m*-H), −2.8 ppm (*o*-H)] and phosphorus ethoxy substituents ($\Delta\delta$ = −3.19 ppm for H_d, −1.49 ppm for H_e, Figure 1) confirm the proximity of these groups to the shielding magnetic field of the porphyrinic macrocycle. For the acetylenic phenyl protons, upfield shifting is much less pronounced ($\Delta\delta$ −0.1 to −0.5 ppm, $H_{a,b,c}$ in Figure 1), as would be expected from the larger distance to the porphyrin core. Lack of a mirror plane in the porphyrin macrocycle renders the α- and β-side of the porphyrin inequivalent, and is expressed in the non-isochronic shifts of the 3′- and 5′-*tert*-butyl groups ($\delta \sim$ 1.5 ppm) and of the 2′- and 4′-*ortho*-protons on the *meso*-phenyl substituents ($\delta \sim$ 7.7 ppm). In [PAP(OEt)$_2$]Ru^{II}(CO)(DPP) (Figure 1), the ethoxy side chains showed additional splitting of the diastereotopic methylene protons into two signals of equal integral value at δ = 0.92 and 0.78 ppm.

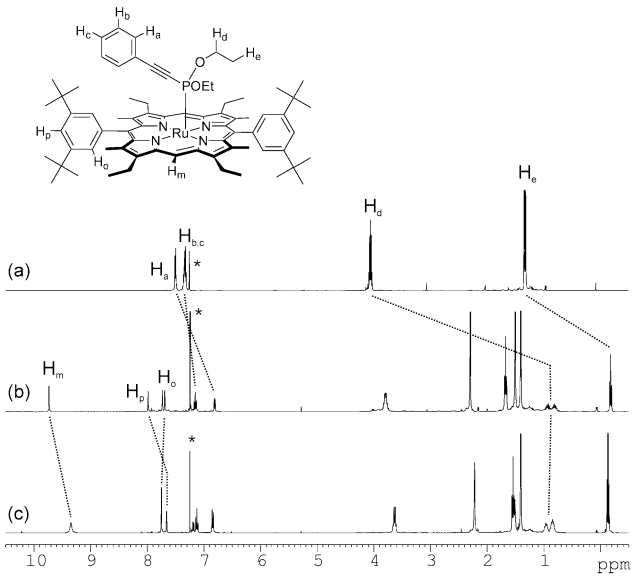

Figure 1. ^{1}H NMR spectra of (a) PAP(OEt)$_2$ (**6**), (b) [PAP(OEt)$_2$]Ru^{II}-(CO)(DPP) (**11**), and (c) [PAP(OEt$_2$)]$_2$Ru^{II}(DPP) (**15**). Dotted lines indicate characteristic chemical shift differences upon ligand binding. Solvent peaks are marked by asterisks (*). Spectra are recorded in $CDCl_3$ (400 MHz) at 25 °C.

Further characteristic chemical shifts were observed in the ^{31}P{^{1}H} NMR spectra (Table 2). Binding of the first phosphorus to ruthenium induces a chemical shift difference $\Delta\delta$, which is +26 ppm for [(PA)$_3$P]Ru^{II}(CO)(DPP), +20 ppm for (DPPA)Ru^{II}(CO)(DPP) and (DPAP)Ru^{II}(CO)(DPP), and −22 ppm for [PAP(OEt)$_2$]Ru^{II}(CO)(DPP) (Figure 2). The chemical shift difference for PPh_3 upon binding is only

(35) Schneider, H.-J.; Yatsimirsky, A. *Principles and Methods in Supramolecular Chemistry*; Wiley-VCH: Weinheim, Germany, 2000.

Table 2. Spectroscopic Data for Ru(CO)(DPP) and the Mono- and Bis-Phosphorus Complexes

		IR $\nu_{C\equiv O}$/cm^{-1} [a]		UV−vis/λ_{max} (log ϵ)[a]			
Ru(CO)(DPP) **2**		1919		400 (5.30); 520 (4.29); 551 (4.25)			
	^{31}P NMR/δ ppm:[b] free ligand (PR$_3$)Ru(CO)(DPP) (PR$_3$)$_2$Ru(DPP)	IR $\nu_{C\equiv O}$/cm^{-1}:[a] (PR$_3$)Ru(CO)(DPP)[b]		UV−vis/λ_{max} (log ϵ):[a] (PR$_3$)Ru(CO)(DPP) (PR$_3$)$_2$Ru(DPP)	K_a/10^{-5} M^{-1}		
ligand PR$_3$			pK_a[c]		K_{a1}[d]	K_{a2}[e]	K_{a3}[f]
DPPA **3**	−32 −12/−32 3/−32	1943		413 (5.09); 533 (4.04); 562 (3.27) 423 (5.25)	12 ± 4	2.5 ± 0.8	37 ± 7
PPh$_3$ **4**	−4 −7 nd[g]	1937	2.73	411 (5.24); 532 (4.31); 559 (3.99)	0.12 ± 0.01		
DPAP **5**	−32 −12 3	1943	1.04	413 (5.12); 533 (4.08); 560 (3.52) 423 (5.44)	12 ± 3	1.5 ± 0.7	19 ± 4
PAP(OEt)$_2$ **6**	130 108 114	1958	6.11	412 (5.01); 532 (3.97); 561 (3.22) 419 (5.64)	48 ± 2	10 ± 3	0.95 ± 0.05
(PA)$_3$P **7**	−85 −59[h] −50[h]	1955	−2.96	412 (4.99); 532 (4.03); 560 (3.52) 418 (5.37)	1.3 ± 0.5		1.5 ± 0.5

[a] In CH_2Cl_2, c = 2.0 mM. [b] In $CDCl_3$. [c] pK_a values are calculated according to literature procedures.[53] [d] Ru(CO)(DPP) + PR$_3$ ⇆ (PR$_3$)Ru(CO)(DPP). [e] Ru(DPP) + PR$_3$ ⇆ (PR$_3$)Ru(DPP). [f] (PR$_3$)Ru(DPP) + PR$_3$ ⇆ (PR$_3$)$_2$Ru(DPP). [g] Not determined. [h] In CD_2Cl_2.

marginal ($\Delta\delta \sim -3$ ppm), accompanied with substantial broadening of the resonance which indicates rapid ligand exchange on the NMR time scale. Most of the phosphorus resonances are also broadened upon complexation, except for [PAP(OEt)$_2$]Ru^{II}(CO)(DPP). For (DPPA)Ru^{II}(CO)(DPP), two resonances can be found in the ^{31}P{^{1}H} NMR spectrum at characteristic values for bound and free phosphine. Using only 0.5 equiv of DPPA to ruthenium porphyrin produced a ^{31}P{^{1}H} NMR spectrum identical to the 1:1 mixture; thus DPPA does not act as a bridging ligand to complex two ruthenium porphyrins.

The mono-phosphine complexes could not be isolated. NMR spectroscopic analysis showed that evaporation of the solvent using a rotary evaporator, or crystallization from the reaction mixture, always yielded the bis-phosphine complexes together with unreacted (MeOH)Ru^{II}(CO)(DPP) in equimolar amounts. The use of carbon monoxide saturated solvents for crystallization gave mainly the mono adducts, but these were always contaminated with 5−15% of the bis-phosphine complexes. All complexes are stable in solution under argon or CO for 1 week. Upon bubbling air through the solutions, significant amounts of phosphine oxides were observed after 2 days, as judged by ^{31}P{^{1}H} NMR spectroscopy. The resonances of the phosphine oxides show a characteristic downfield shift as compared to the phosphine, e.g., $\Delta\delta = +41$ ppm for the oxidized DPAP; contrarily, the phosphonate resonance is shifted upfield by 135 ppm compared to the phosphonite.

Broadening of the ^{1}H and ^{31}P{^{1}H} NMR signals of the ligands in (PR$_3$)Ru^{II}(CO)(DPP) and UV−vis spectroscopy indicates a dynamic ligand exchange in both mono- and bis-phosphorus complexes. This was confirmed first by exchange experiments involving mixtures of different phosphines in solution, e.g., exchange of (PA)$_3$P with DPAP on (PR$_3$)Ru^{II}(CO)(DPP) (data not shown), and second by diagnostic NOESY exchange peaks of the phenyl proton signals in (DPPA)Ru^{II}(CO)(DPP) (Figure 3.) Through-space NOEs between the para protons $H_c \leftrightarrow H_f$, which are more than 5 Å apart, are not expected. Thus the two phosphines in DPPA are exchangeable upon complexation to ruthenium at a rate which is slow on the chemical shift time scale, but fast on the NOE and relaxation (R_1) time scale.[36] Whether this exchange is a simple dissociation−reassociation process[37,38] or if an alkyne bound transition state is present[39] remains unclear. A similar kinetic lability was also observed in other ruthenium(II)[25] and platinum(II) phosphine complexes on the basis of ^{31}P{^{1}H} NMR spectroscopy[40] and explains the difficulties encountered in isolating the mono-phosphine complexes. To our knowledge, such an exchange has not previously been directly observed using 2D NMR spectroscopy.

IR Spectroscopy. Also summarized in Table 2 are ruthenium C≡O triple bond IR stretching frequencies. The spectra were recorded using 2.0 mM solutions in methylene chloride. $\nu_{C\equiv O}$ in (PR$_3$)Ru^{II}(CO)(DPP) is shifted to higher wavenumbers compared to (MeOH)Ru^{II}(CO)(DPP), the differences varying from 18 cm^{-1} for PPh$_3$ to 39 cm^{-1} for PAP(OEt)$_2$ (Figure 4). The relative intensities of the IR absorptions decrease with increasing ν, and the half-widths of the peaks increase with the same trend. The $\nu_{C\equiv O}$ band in (MeOH)Ru^{II}(CO)(DPP) shows a half-width of 19 cm^{-1}, while the band corresponding to [PAP(OEt)$_2$]Ru^{II}(CO)(DPP) has a half-width of 31 cm^{-1} and a 50% decreased intensity. (DPAP)Ru^{II}(CO)(DPP) and (DPPA)Ru^{II}(CO)(DPP) displayed the same IR spectra in the $\nu_{C\equiv O}$ region. $\nu_{C\equiv O}$ for the parent Ru^{II}(CO)(DPP) is independent on whether the bound ligand

(36) Sanders, J. K. M.; Hunter, B. K. *Modern NMR Spectroscopy*, 2nd ed.; Oxford University Press: Oxford, 1993.
(37) James, S. L.; Lozano, E.; Nieuwenhuyzen, M. *Chem. Commun.* **2000**, 617.
(38) Clark, H. C.; Ferguson, G.; Kapoor, P. N.; Parvez, M. *Inorg. Chem.* **1985**, *24*, 3924.
(39) (a) Lee, H. M.; Bianchini, C.; Jia, G. C.; Barbaro, P. *Organometallics* **1999**, *18*, 1961. (b) Ihmels, K.; Rehder, D. *Organometallics* **1985**, *4*, 1334.
(40) Romeo, R.; Alibrandi, G. *Inorg. Chem.* **1997**, *36*, 4822.

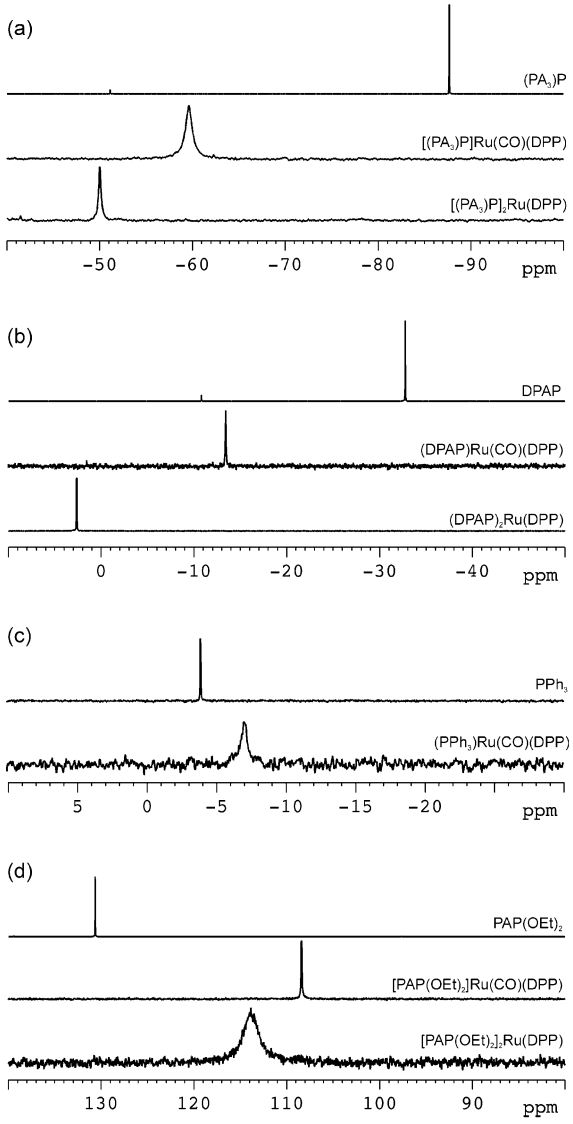

Figure 2. $^{31}P\{^1H\}$ NMR spectra of the free ligands (top), mono-phosphine complexes (middle), and bis-phosphine complexes (bottom): (a) $(PA)_3P$; (b) DPAP; (c) PPh_3; (d) $PAP(OEt)_2$. Spectra are recorded in $CDCl_3$ (162 MHz) at 25 °C.

is MeOH or THF. As the ruthenium porphyrin is crystallized from $CHCl_3$−MeOH after synthesis, and obtained as the MeOH solvate, this additional ligand is therefore readily displaced, and does not interfere with the binding of the phosphorus ligand. Analogous observations were made previously when pyridine ligands were complexed to Ru(II) porphyrins.[41]

Synthesis and NMR Spectroscopy of Bis-Phosphine Complexes. The bis-phosphine complexes $(DPAP)_2Ru^{II}(DPP)$, $(DPPA)_2Ru^{II}(DPP)$, $[(PA)_3P]_2Ru^{II}(DPP)$, and $[PAP(OEt_2)]_2$-$Ru^{II}(DPP)$ (Chart 3) are easily accessible by mixing 5 equiv of the phosphine with $(MeOH)Ru^{II}(CO)(DPP)$ and evaporating the solvent. Extensive boiling in $CHCl_3$ or toluene as for the PPh_3 complexes is not required. Recrystallization from hot chloroform−methanol mixtures gave the complexes in high yield and purity.

(41) (a) Webb, S. J.; Sanders, J. K. M. *Inorg. Chem.* **2000**, *39*, 5920. (b) Webb, S. J.; Sanders, J. K. M. *Inorg. Chem.* **2000**, *39*, 5912.

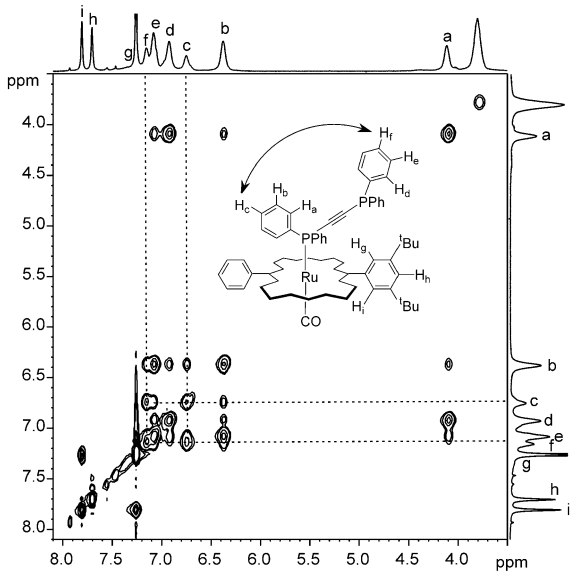

Figure 3. Aromatic region of the NOESY spectrum of $(DPPA)Ru^{II}(CO)$-(DPP) in $CDCl_3$. The signal of H_g in the one-dimensional spectrum is masked by the $CHCl_3$ resonance.

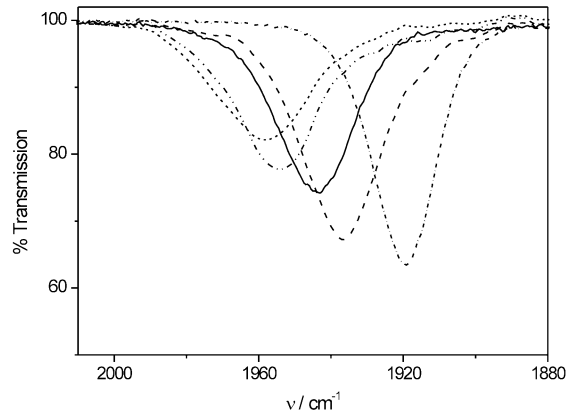

Figure 4. IR spectra of the mono-phosphine complexes $(MeOH)Ru^{II}(CO)$-(DPP) (-·--·), $(PPh_3)_2Ru^{II}(DPP)$ (− − −), $[(PA)_3P]_2Ru^{II}(DPP)$ (-···-···), $(DPAP)_2Ru^{II}(DPP)$ and $(DPPA)_2Ru^{II}(DPP)$ (—), and $[PAP(OEt_2)]_2Ru^{II}(DPP)$ (---). Shown is the wavenumber region of the carbonyl stretching absorption. Spectra are recorded in CH_2Cl_2 at 2.0 mM concentration of $(MeOH)Ru^{II}$-(CO)(DPP) and ligand.

The ^1H NMR shifts of the ligands are similar to those of the mono-phosphine complexes, but are generally sharper and better resolved (Figure 1). On the porphyrin moiety, shift differences are observed for the *meso*-protons ($\Delta\delta$ 0.41 to 0.59 ppm, H_m in Figure 1), and for the *meso*-phenyl substituents ($H_{o,p}$ in Figure 1). Due to the higher symmetry compared to the mono-phosphine complexes, the resonances of the 3′- and 5′-*tert*-butyl groups and of the 2′- and 4′-*ortho*-protons on the *meso*-phenyl substituents become isochronous.

The phosphorus chemical shifts are significantly different in the bis-phosphine complexes compared to the mono complexes. The shift differences (Table 2), compared to the free ligands, are +35 ppm for $[(PA)_3P]_2Ru^{II}(DPP)$, $(DPAP)_2$-$Ru^{II}(DPP)$, and $(DPPA)_2Ru^{II}(DPP)$, but −16 ppm for $[PAP$-$(OEt_2)]_2Ru^{II}(DPP)$ (Figure 2). Also, the signals are sharper than for the monomeric counterparts, except for $[PAP$-$(OEt_2)]_2Ru^{II}(DPP)$, which showed a broadened signal.

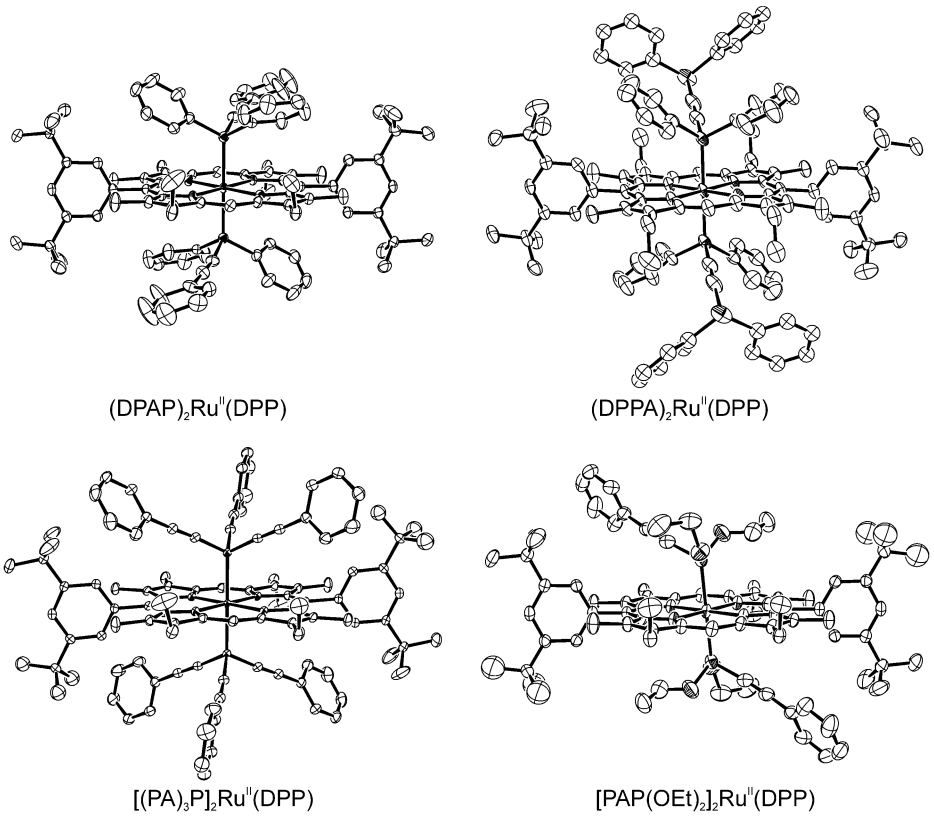

Figure 5. Molecular units in the bis-phosphine complexes showing displacement ellipsoids at the 50% probability level. For $(DPAP)_2Ru^{II}(DPP)$, only the triclinic structure of the polymorphic structures is shown. For $(DPPA)_2Ru^{II}(DPP)$, only one of the disordered geometries of the unbound phosphine group is displayed. H atoms are omitted for clarity.

X-ray Structures. The bis-phosphine complexes formed deep orange to bronze colored single crystals overnight from chloroform solutions layered with methanol. All complexes crystallize with the Ru atom sited at a crystallographic center of symmetry such that the molecular units are centrosymmetric. $[(PA)_3P]_2Ru^{II}(DPP)$, $[PAP(OEt)_2]_2Ru^{II}(DPP)$, and $(DPAP)_2Ru^{II}(DPP)$ crystallize in space group $P\bar{1}$. The crystals of $[(PA)_3P]_2Ru^{II}(DPP)$ also contain chloroform molecules (four per molecular unit). Two of the three structures, $[(PA)_3P]_2Ru^{II}(DPP)$ and $[PAP(OEt)_2]_2Ru^{II}(DPP)$, display disorder of the *tert*-butyl groups, and these were modeled in two orientations with a single isotropic displacement parameter common to all C atoms. $(DPPA)_2Ru^{II}(DPP)$ crystallizes in the orthorhombic space group *Pccn* with four molecules in the unit cell.[62] The phenyl substituents of the DPPA unit display some disorder, and these were modeled in two orientations. The four molecular units of the complexes are shown in Figure 5.

For $(DPAP)_2Ru^{II}(DPP)$, the majority of crystals were large orange blocks (the triclinic form), but small orange plates of a second polymorph (the monoclinic form) were also observed in the bulk material. The crystals of this monoclinic form were small and weakly diffracting, but it was possible to determine their structure using a synchrotron radiation source. This polymorph crystallizes in the space group *C*2/*c* with four molecules in the unit cell. The data are relatively poor, however (R_{int} ca. 20%), and refinement of the structure was problematic; it was possible only to refine all atoms with isotropic displacement parameters. The alkynylphenyl substituents of the DPAP unit display some disorder and were modeled in two orientations with the rings constrained to be true hexagons (Figure 6).

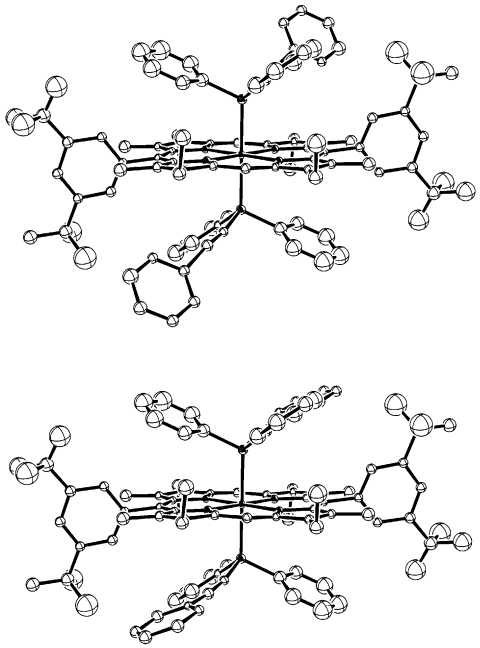

Figure 6. Disordered molecular units of the monoclinic crystal structure of $(DPAP)_2Ru^{II}(DPP)$. Isotropic spheres are shown at the 30% probability level. H atoms are omitted.

Calculated geometrical parameters are summarized in Table 3. The geometrical parameters (Figure 7) of the

Table 3. Selected Geometrical Data for the Solid State Structures of the Bis-Phosphorus Complexes[a]

	$(DPAP)_2Ru^{II}(DPP)$ (**12**)			$(DPPA)_2Ru^{II}(DPP)$ (**13**)				
		monoclinic			P unbound		$[(PA)_3P]_2$-$Ru^{II}(DPP)$ (**14**)	$[PAP(OEt_2)]_2$-$Ru^{II}(DPP)$ (**15**)
	triclinic	isomer 1	isomer 2	P bound	conformer 1	conformer 2		
σ/Å	0.026	0.067		0.047			0.042	0.038
Ru−N1/Å	2.061(3)	2.067(14)		2.063(4)			2.0642(17)	2.067(2)
Ru−N2/Å	2.063(3)	2.079(13)		2.053(2)			2.0621(16)	2.068(2)
Φ(Por-Ar_{meso})/deg	81.9	73.8		79.2			86.2	82.8
d(Ru−P)/Å	2.3623(10)	2.340(5)		2.334(2)			2.297(5)	2.3140(8)
γ(RuP-por)/deg	89.50	77.4		84.75			87.64	85.47
Ω/deg	132.1	127.7	126.3		124.6	121.7	144.9	127.9
θ/deg		145			145		145	121
l(P−$C_{\equiv}$)/Å	1.757(4)	1.758(18)		1.776(3)	1.779(3)	1.827(5)	1.759(2); 1.759(2); 1.755(2)	1.774(4)
Φ(RuPC−$Ar_{C\equiv}$)/deg	72.9	71.1	48.2				7.8; 13.1; 46.7	34.8
l(P−CPh_1/O_1)/Å	1.837(4)	1.820(11)		1.834(1)	1.955(4)	1.870(2)		1.592(2)
Φ(RuPC−Ph_1)/deg Φ(O2−P−O1−C)/deg	76.3	74.6		55.2	86.4	74.3		−55.6
l(P−CPh_2/O_2)/Å	1.830(4)	1.862(14)		1.827(2)	1.859(3)	1.849(2)		1.643(3)
Φ(RuPC−Ph_2)/deg Φ(O1−P−O2−C)/deg	58.2	68.3		74.9	57.3	63.5		61.3
φ(P−C≡C)/deg	169.1(4)	170.1(17)			172.9	173.6	177.10(19); 176.4(2); 175.1(2)	173.5

[a] For assignments, see text and Figure 7.

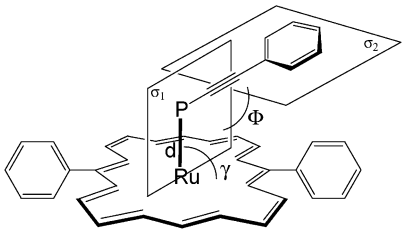

Figure 7. Definition of selected geometrical parameters. Φ indicates the dihedral angle between the least-squares planes (σ_1, σ_2) schematically shown as rectangles. σ_1 is defined by the atoms Ru, P, and C(acetylene); σ_2 is defined by the aryl group attached to the acetylene unit.

phosphines such as the Ru−P bond lengths (d), the angle between the Ru−P bond and the porphyrin plane (γ), the crystallographic cone angles (Ω), and dihedral angles (Φ) between the plane Ru−P−C (σ_1) and the alkynylphenyl mean plane (σ_2) show characteristic values for the individual structures; these are discussed below. Ω values were determined according to Mingos's procedure,[23] but using the true crystallographic Ru−P bond lengths (d) instead of a normalized value.

UV−Vis Spectroscopy and Binding Constants. Standard UV−vis titration methods (10^{-6} M solutions) to determine directly the first and second binding constants using the B-band absorption (∼400 nm) as well as the Q-band absorptions (500−600 nm) failed for these systems, because no isosbestic points could be observed, and the data-fitting was not reproducible. The reason for this behavior is irreversible loss of CO upon addition of a large excess of ligand, leading to a complex equilibrium system according to Scheme 1 (vide infra). To determine the first association constant, the use of rather concentrated solutions (10^{-4} M **2**), and titrating 0.1 equiv of phosphine, showed a hypochromic shift in the absorption maxima, in both the B-band and Q-band regions (see Table 2). Isosbestic points were observed when no more than 1.2 equiv of phosphine was added. The data were fitted to a model assuming a single binding event, according to eq 4,

$$(MeOH)Ru^{II}(CO)(DPP) + PR_3 \rightleftarrows (PR_3)Ru^{II}(CO)(DPP) \quad (4)$$

where PR_3 is the corresponding phosphine. Using eq 1 (see Experimental Section), a nonlinear least-squares fitting procedure was applied to the changes in the molar extinction coefficient at 400, 411, 520, 534, and 551 nm. Figure 8 shows the curves obtained for the decrease at 520 nm. Due to possible partial loss of CO during the titrations, the standard deviations shown in Table 2 may underestimate the uncertainty in the binding constant determination. An exception was found when titrating PPh_3 to $(MeOH)Ru^{II}(CO)$-(DPP): the spectra showed isosbestic points when using 10^{-5} M $(MeOH)Ru^{II}(CO)(DPP)$ solutions, and the first binding constant was determined via standard calculations (Table 2).

The second binding constants were determined using dilution experiments of the bis-phosphine complexes. After a baseline correction, a Gaussian deconvolution of the absorption bands was possible when assuming that three different species with absorption maxima at 400 nm [Ru^{II}-(DPP)], ∼411 nm [$(PR_3)Ru^{II}(DPP)$], and ∼420 nm [$(PR_3)_2$-$Ru^{II}(DPP)$] are present (Figure 9). For $[(PA)_3P]Ru^{II}(CO)$-(DPP), the UV−vis spectra could not be deconvoluted using the three-component model, but assuming the presence of only the mono- and bis-phosphine complexes. Only the B-band absorptions could be used in the calculations, because the low-energy absorption of the bis-complexes is very broad, and no distinct Q-band absorptions could be observed. This is discussed in the following paper.[61]

The maxima assigned to $Ru^{II}(DPP)$ and $(PR_3)Ru^{II}(DPP)$ were found at the same values as were obtained by direct measurement of the corresponding CO-containing complexes. Under the assumption that the dissociated species have similar extinction coefficients as the CO-containing complexes (based on the same λ_{max} values), and from the known total concentration of porphyrin, the dissociation constants were calculated according to equilibria 2 and 3 (see Experimental Section).

Scheme 1

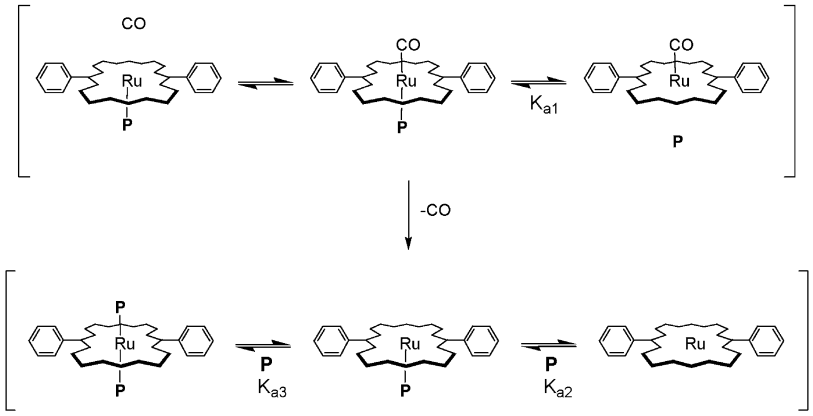

Discussion

Synthesis and Reactivity in Solution. The rapid complexation of phosphines and phosphonates to $Ru^{II}(CO)$ porphyrins has been reported earlier.[15,17,18,21,42] Upon mixing equimolar amounts of alkynyl phosphorus ligands with $(MeOH)Ru^{II}(CO)(DPP)$, ^1H and $^{31}P\{^1H\}$ NMR spectra showed rapid and complete formation of the mono-phosphorus complexes in the millimoles per liter range. The spectra are significantly different from those obtained with PPh_3; this ligand does not bind strongly to $(MeOH)Ru^{II}(CO)(DPP)$ ($K_a = 1.2 \times 10^4\ M^{-1}$), as is clear from the broadened $^{31}P\{^1H\}$ NMR resonances (Figure 2). PPh_3 complexes of $Ru^{II}(OEP)$ ($K_a = 8.3 \times 10^4\ M^{-1}$) and $Ru^{II}(TPP)$ ($K_a = 7.4 \times 10^3\ M^{-1}$) were also reported to dissociate in solution.[15] The bis-phosphine complexes are readily accessible using an excess of ligand and evaporating the solvent. A single crystallization step gives the pure product in high yield. The ligands therefore weaken the *trans*-CO sufficiently that it can be removed simply by applying low pressure. This is in contrast to triaryl phosphines, for which prolonged heating in $CHCl_3$ or toluene is required to form the bis-complexes. The ^1H NMR spectra for $(PR_3)Ru^{II}(CO)(DPP)$ and $(PR_3)_2Ru^{II}(DPP)$ were very similar with respect to the chemical shifts, but the $^{31}P\{^1H\}$ NMR spectra allowed unambiguous assignment of the complexes due to their distinctive δ values.

Rotational flexibility around the Ru−P bond and P−C bonds in solution, judged from the equivalence of the β-pyrrole substituents and the phosphorus phenyl substituents in the ^1H NMR spectra, leads the complexes to have higher C_{2v} symmetry (mono-P complex) or D_{2h} symmetry (bis-P complex) than the crystallographic C_1 or C_i symmetry, respectively. This higher symmetry has no effect on the inequivalency of the α- and β-sides of the porphyrin in the $(PR_3)Ru^{II}(CO)(DPP)$ complexes, which is expressed in different chemical shifts of the *meso*-phenyl protons.[7,43] NOESY exchange peaks $H_g \leftrightarrow H_i$ (Figure 3) indicate, however, that slow spinning with respect to the NMR chemical shift time scale around the *meso*-aryl bond is occurring in solution.

Despite their lability, the mono-phosphine complexes are the kinetic products, as addition of up to 1.2 equiv of phosphine did not yield detectable amounts of higher complexes after 2 days ($^{31}P\{^1H\}$ NMR.) Only after heating was formation of the bis-complex detected. Extensive bubbling of CO through solutions of $(PR_3)_2Ru^{II}(DPP)$ in chloroform did not result in a clean back-conversion to $(PR_3)Ru^{II}(CO)(DPP)$ as occurs with ferrous porphyrins.[11] We therefore conclude that, in solution, all complexes exist in a dynamic equilibrium according to Scheme 1.

Solid State Structures and Cone Angles. The crystal structures of the bis-phosphine complexes, as shown in Figure 5, allow direct comparison of the differences in geometry upon variation of the phosphorus substituents. Common to all structures is the centrosymmetry (i = Ru). Even though significant ruffling could occur because of the strong M→P π-back-bonding,[10] the porphyrin cores display relatively little ruffling. The porphyrin planes are essentially flat, the mean deviation σ from planarity being in the range of 0.026 Å for the triclinic form of $(DPAP)_2Ru^{II}(DPP)$ to 0.067 Å for the monoclinic form of $(DPAP)_2Ru^{II}(DPP)$. The mean plane was defined using all 24 atoms of the porphyrin core and the Ru^{2+} center. Tilting of the *meso*-phenyl groups in all structures is within a small range of about 10° from orthogonality. Such an arrangement minimizes steric interactions with the methyl groups at the β-pyrrole positions in the solid state.

The acetylene substituent of the ligands has a tendency to adopt an approximately eclipsed orientation (ligand over nitrogen), especially in $(DPAP)_2Ru^{II}(DPP)$ (both monoclinic and triclinic forms), $[(PA)_3P]_2Ru^{II}(DPP)$, and $[PAP(OEt_2)]_2Ru^{II}(DPP)$. One of the remaining substituents (phenyl, alkynylphenyl, ethoxy) in these structures is also eclipsed. The ligands are oriented such that the alkynylphenyl group is located toward the unsubstituted *meso*-carbon. Only in $(DPPA)_2Ru^{II}(DPP)$ does the phosphine adopt a clear staggered conformation over the free *meso* position, the phosphine phenyl groups being located directly above the pyrrole nitrogens. The configurations of the ethoxy groups in $[PAP(OEt_2)]_2Ru^{II}(DPP)$ are similar to those found in Fe(III) porphyrin complexes of $PhP(OEt)_2$.[10] As the ^1H NMR spectra indicate, however, the ligands have no preferred geometry in solution.

(42) Cheng, P. C.; Liu, I. C.; Hong, T. N.; Chen, J. H.; Wang, S. S.; Wang, S. L.; Lin, J. C. *Polyhedron* **1996**, *15*, 2733.
(43) Abraham, R. J.; Marsden, I. *Tetrahedron* **1992**, *48*, 7489.

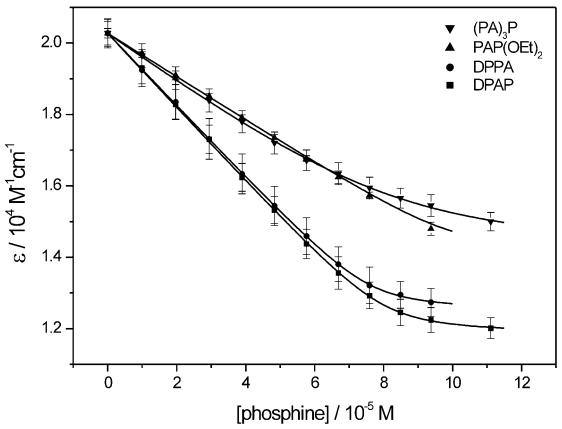

Figure 8. Decrease of porphyrin molar extinction coefficient at $\lambda = 520$ nm, obtained from titration experiments; CH_2Cl_2, 25 °C, [**2**] $= 10^{-4}$ M.

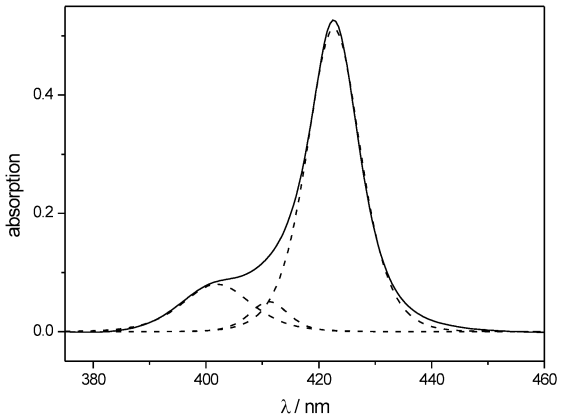

Figure 9. B-band absorption region of $(DPAP)_2Ru^{II}(DPP)$ (—) and deconvolution (– – –) after baseline correction; CH_2Cl_2, 25 °C, $c = 2.6 \times 10^{-5}$ M.

The acetylene units show deviation from linearity with torsion angles φ(P−C≡C) varying from 169.1(4)° to 177.10(19)° (Table 3). Such deviation is usually observed in μ_2-DPPA complexes and stems from strain or steric crowding.[37,38,44] In the complexes considered here, the deviation might arise from crystal packing forces, as the C≡CPh units are bent toward the aromatic macrocycle. The Ru−P bond lengths *d* are clearly shorter [2.297(5)−2.3623(10) Å] than those found for $Ru-PPh_3$ complexes, which have an average value of 2.428 Å in TPP and OEP.[15] This is in agreement with the higher binding constants obtained for the alkynyl phosphorus ligands.

The calculated cone angles (Tolman's cone angle θ)[22] and the crystallographically determined cone angles (solid angle Ω)[23] do not match for most of the complexes (Table 3). This trend has been observed previously in systematic analyses of phosphine complexes using crystallographic databases.[23,45,46] Even though variations in Ω of about 30° for a specific phosphine ligand in variable environments are common, the mean values of all Ω's usually coincide with θ.[23] The θ values of our ligands show that introducing an alkyne spacer between the phosphorus and the aryl substituent does not alter the half-angle of the ligand. DPAP, DPPA, and $(PA)_3P$ display the same calculated steric demand as PPh_3 ($\theta = 145°$), which clearly is not reflected in the thermodynamic stability of the complexes, because the alkyne phosphines display a much higher association constant compared to PPh_3. Only $PAP(OEt)_2$ has a smaller θ and a correspondingly larger K_{a1} value.

Systematic Cambridge structural database searches[47] revealed that crystal packing forces may lead to distortions, and standard deviations (σ) of M−P bond lengths and torsion angles Φ(M−P−Ph) (Figure 7) can be as high as 0.02 Å and >40°, respectively. The Ru−P bond lengths *d* in our structures are within a range of ±0.03 Å. Inspection of the dihedral angles Φ in the different structures (Table 3) shows that Φ for the phosphine phenyl substituents varies from 55.2° to 86.4°. The alkynylphenyl substituents have an even greater flexibility, showing values from 7.76° to 72.94°. As θ is influenced by both Φ(PPh) and Φ(PC≡CPh), and as Φ has an apparently independent variation from the overall relative conformation, Ω varies accordingly. For $(DPAP)_2Ru^{II}(DPP)$ and $(DPPA)_2Ru^{II}(DPP)$, Ω values are about 15−20° smaller than θ; for $[(PA)_3P]_2Ru^{II}(DPP)$ and $[PAP(OEt_2)]_2Ru^{II}(DPP)$ the calculated and measured values match reasonably well.

Stereoelectronic Effects. Stereoelectronic effects have strong influence on stability and reactivity of transition metal phosphorus complexes, and a fine balance between σ-donation and π-acceptance defines the overall physical properties. Stereoelectronic effects are influenced by both the type of the substituents on the phosphorus (electronegativity, π-delocalization) and the dihedral angles C−P−C, reflecting steric effects of the ligand (θ). The qualitative influence of σ/π- and θ-parameters on the reactivity of phosphorus ligands remains hotly debated.[46,48−50] To date, there is little information available from spectroscopic studies involving acetylenic phosphines,[27,28] and only DPPA has gained significant attention because of its ability to act as a bridging ligand to form cage type structures.[37,44,51,52]

Since the pK_a of HPR_3^+ is free of π-back-bonding effects, the basicity of the phosphorus is an attractive measure of the σ-donor strength.[24] The pK_a values of the ligands in our series were calculated using the substituent parameters

(44) (a) Semmelmann, M.; Fenske, D.; Corrigan, J. F. *J. Chem. Soc., Dalton Trans.* **1998**, 2541. (b) Amoroso, A. J.; Johnson, B. F. G.; Lewis, J.; Massey, A. D.; Raithby, P. R.; Wong, W. T. *J. Organomet. Chem.* **1992**, *440*, 219.
(45) (a) Smith, J. M.; Coville, N. J.; Cook, L. M.; Boeyens, J. C. A. *Organometallics* **2000**, *19*, 5273. (b) White, D.; Taverner, B. C.; Coville, N. J.; Wade, P. W. *J. Organomet. Chem.* **1995**, *495*, 41. (c) Smith, J. M.; Taverner, B. C.; Coville, N. J. *J. Organomet. Chem.* **1997**, *530*, 131.
(46) Smith, J. M.; Coville, N. J. *Organometallics* **2001**, *20*, 1210.
(47) Martin, A.; Orpen, A. G. *J. Am. Chem. Soc.* **1996**, *118*, 1464.
(48) (a) Bubel, R. J.; Douglass, W.; White, D. P. *J. Comput. Chem.* **2000**, *21*, 239. (b) Fernandez, A.; Reyes, C.; Prock, A.; Giering, W. P. *Organometallics* **1998**, *17*, 2503. (c) Fernandez, A. L.; Lee, T. Y.; Reyes, C.; Prock, A.; Giering, W. P.; Haar, C. M.; Nolan, S. P. *J. Chem. Soc., Perkin Trans. 2* **1999**, 2631. (d) Woska, D.; Prock, A.; Giering, W. P. *Organometallics* **2000**, *19*, 4629. (e) Joerg, S.; Drago, R. S.; Sales, J. *Organometallics* **1998**, *17*, 589.
(49) Joerg, S.; Webster, C. E.; Drago, R. S.; Sales, J. *Polyhedron* **1999**, *18*, 1097.
(50) Bosque, R.; Sales, J. *J. Chem. Inf. Comput. Sci.* **2001**, *41*, 225.
(51) Hui, B. K. M.; Wong, W. T. *J. Chem. Soc., Dalton Trans.* **1998**, 447.
(52) Layer, T. M.; Lewis, J.; Martin, A.; Raithby, P. R.; Wong, W. T. *J. Chem. Soc., Dalton Trans.* **1992**, 3411.

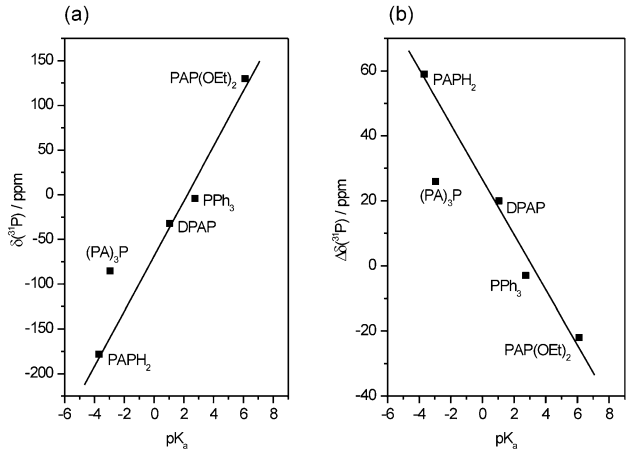

Figure 10. Correlation between the calculated[53] pK_a values of the ligands and (a) the phosphorus chemical shift resonance $\delta(^{31}P)$ or (b) the phosphorus chemical shift differences $\Delta\delta(^{31}P) = \delta(^{31}P)_{mono-phosphine} - \delta(^{31}P)_{free\ phosphine}$. Straight lines are linear regressions [R(δ) = 0.994, R($\Delta\delta$) = 0.992].

reported in the literature (except for PPh_3).[53] The electronic and steric properties of phosphines have been correlated with $^{31}P\{^1H\}$ NMR chemical shifts in order to predict the chemical shifts of phosphines.[50,54] Our data show a linear dependence of the pK_a vs $\delta(^{31}P)$ (Figure 10), even if the primary (phenylacetenyl)phosphine ($PAPH_2$)[55] is included in the analysis.[63] $(PA)_3P$ was excluded from the calculation of the linear regression. This outlier indicates that the $\delta(^{31}P)$ value might also be influenced by electronic factors other than the (calculated) pK_a. More interestingly, the $\Delta\delta(^{31}P)$ values of $(PR_3)Ru^{II}(CO)(DPP)$ compared to the free ligands also correlate linearly with the pK_a of the phosphine,[64] and $(PA)_3P$ again is an outlier. Based on the $\Delta\delta$-regression, the calculated and measured $\Delta\delta(^{31}P)$ values show a linear correlation with a slope of 1.06, confirming the validity of the regression. Therefore we propose that the pK_a of a specific phosphorus ligand can be estimated on the basis of the chemical shift difference $\Delta\delta(^{31}P)$ upon complexation to $(MeOH)Ru^{II}(CO)$-(DPP), or to any other metalloporphyrin. The analyzed system spans a very large range both on the phosphorus NMR scale ($\delta = -178$ to $+130$ ppm) and on the pK_a scale (-3.96 to $+6.11$) and seems representative. This approach is the reverse of the previously reported correlations, because we are suggesting the use of the $^{31}P\{^1H\}$ NMR chemical shift to probe the electronic properties of the phosphorus.

π-Back-bonding in phosphorus complexes is assumed to increase with decreasing σ-donation.[49] The IR shifts of the carbonyl stretching frequency ($\nu_{C\equiv O}$) are among the most diagnostic probes to elucidate the bonding in metal complexes.[18,51,56] $\nu_{C\equiv O}$ is correlated to both σ- and π-effects: σ-donation increases the electron density on the metal, strengthens the Ru−CO bond by increased π-back-bonding to CO, and lowers the energy of the carbonyl triple bond, which is expressed in an overall decreased stretching frequency. π-Acceptance has an opposite effect and weakens the Ru−CO bond. In the following section, both σ- and π-effects are discussed individually for each type of ligand (triarylphosphine, alkynylphosphine, phosphonite).

PPh_3, being the second strongest base (p$K_a = 2.73$) among the ligands in our series and consequently a relatively strong σ-donor, displays the smallest IR shift of all complexes ($\Delta\nu = 18$ cm^{-1}), which suggests that the π-acceptor ability is weak.[27] The $^{31}P\{^1H\}$ NMR resonance of the mono-complex is very broad (vide supra), indicating rapid exchange between free and bound species at a rate comparable to the NMR chemical shift time scale. These observations are consistent with the lowest association constant measured ($K_{a1} = 1.2 \times 10^5$ M^{-1}), and with the long Ru−P bonds of porphyrin phosphine complexes determined from the related TPP and OEP systems. A threshold of d(Ru−P) = 2.40 Å was suggested for stable phosphine complexes,[15] which is exceeded in PPh_3 porphyrin complexes. Existence of the $(PPh_3)_2Ru^{II}$(DPP) complex in solution could not be confirmed by NMR spectroscopy. The association constant K_{a1} is between the values found for Ru^{II}(TPP) (7.4×10^3 M^{-1}) and Ru^{II}(OEP) (8.3×10^4 M^{-1})[15] and suggests hybrid properties of DPP compared to TPP and OEP. Since axial binding to metalloporphyrins is also influenced by the basicity of the porphyrin core, $K_{a1}(PPh_3)$ allows an estimation of the pK_a of DPP to be in the range of the values found for OEP (pK_a ~3) and TPP (pK_a ~6).[15,18]

Generally, the substitution of phenyl groups in PPh_3 by phenylacetylene groups induces changes in the ligand properties which have a large influence on the reactivity of the phosphines. Most remarkable are the incrementally decreased basicity [pK_a(DPAP) = 1.04, pK_a({PA}$_3$P) = −2.96], higher association constants (Table 2), and relative ease of formation of the bis-phosphine complex (weakening of the Ru−CO bond through enhanced π-back-bonding).[51] The larger $\Delta\nu_{C\equiv O}$ values for DPAP, DPPA, and $(PA)_3P$ compared to PPh_3 are due to an increased π-acidity as well as to a decreased σ-donor strength of the ligands.[27,28] The increase in π-acceptor ability can be explained either by delocalization into π^*(C≡C) orbitals or by electronic communication via the ethynyl linker to the phenyl ring, leading to enhanced delocalization. The stronger π-back-bonding also leads to a decrease in the Ru−P bond lengths[27] compared to the PPh_3 complexes of TPP and OEP, consistent with the higher association constants. The $^{31}P\{^1H\}$ NMR shifts from the free to the bound ligands upon first binding indicate a relatively large decrease in electron density around the phosphorus in the complexes, which is not compensated by simultaneous Ru→PR_3 π-back-bonding. Upon decarbonylation, the DPP is expected to have enhanced metal-to-porphyrin (M→por) π-back-bonding, increasing its charge density at the expense of the PR_3→M σ-donation.[57] The metal therefore becomes a stronger Lewis acid, reducing the net

(53) (a) Henderson, W. A.; Streuli, C. A. *J. Am. Chem. Soc.* **1960**, *82*, 5791. (b) Allman, T.; Goel, R. G. *Can. J. Chem.* **1982**, *60*, 716.
(54) Abdur-Rashid, K.; Fong, T. P.; Greaves, B.; Gusev, D. G.; Hinman, J. G.; Landau, S. E.; Lough, A. J.; Morris, R. H. *J. Am. Chem. Soc.* **2000**, *122*, 9155.
(55) Guillemin, J. C.; Savignac, P.; Denis, J. M. *Inorg. Chem.* **1991**, *30*, 2170.
(56) Vogel, K. M.; Kozlowski, P. M.; Zgierski, M. Z.; Spiro, T. G. *Inorg. Chim. Acta* **2000**, *297*, 11.
(57) (a) Buchler, J. W.; Kokisch, W.; Smith, P. D. *Struct. Bonding* **1978**, *34*, 79. (b) Gross, Z.; Mahammed, A.; Barzilay, C. M. *Chem. Commun.* **1998**, 1105.

charge density on the phosphorus in $(PR_3)_2Ru^{II}$(DPP) compared to $(PR_3)Ru^{II}$(CO)(DPP), and resulting overall in a larger downfield shift of the $^{31}P\{^1H\}$ NMR resonance. This demonstrates the large trans influence of ligands on both stability and chemical shifts.[11]

Attachment of a phosphorus at the alkynyl substituent in DPPA was expected to alter the overall affinity to (MeOH)-Ru^{II}(CO)(DPP). We intended to detect possible π-interactions between the bound and the free phosphorus by spectroscopic differences to DPAP.[28] As the $^{31}P\{^1H\}$ NMR chemical shifts and $\Delta\nu_{C\equiv O}$ show, however, there is no alteration in the overall stereoelectronic properties. The K_{a1} value does not show a 2-fold increase in value which would be expected if two phosphines were acting independently, doubling the effective ratio k_{assoc}/k_{diss}. The solid state structure shows that the second phosphine orients its lone pair toward the porphyrin core, in accordance with the conformation necessary for intramolecular exchange in solution. This preferred conformation might explain why DPPA does not act as a bridging ligand, as is observed with other transition metal complexes, and $^{31}P\{^1H\}$ NMR spectroscopy shows signals for one bound and one free phosphorus.[58] K_{a3} increases about 2-fold on changing from DPAP to DPPA, which is not consistent with the observations for the mono-phosphine complex. The spectroscopic data suggest that there is indeed no electronic communication between the two phosphines through the acetylenic spacer.

The phosphonite $PAP(OEt)_2$ has the highest $^{31}P\{^1H\}$ NMR chemical shift ($\delta = +130$ ppm); thus the nucleus of the phosphorus is strongly deshielded, which is attributed to the polarized P−O bond. $PAP(OEt)_2$ is the strongest base ($pK_a = +6.11$) of all our investigated ligands, contrary to the expected decrease in basicity due to the electronegative ethoxy substituents.[13] Despite this high basicity, the largest shift in the IR spectrum is observed ($\Delta\nu = +39$ cm^{-1}), consistent with the known π-acidity of phosphonites.[10,11,25] This is a common feature of the P−O substitution pattern and can best be seen in the relative bond lengths of the related phosphate group, where the P−O(C) bonds have partial double bond character, attributed to P(3d)−O(2pπ/2pπ*) orbital interactions.[59] Whereas all phosphinoalkyne ligands display a downfield shift upon complexation, in the case of $PAP(OEt)_2$ the electron density around the phosphorus nucleus increases, leading to a net upfield shift of the resonance. This indicates that the energetic contribution of the π-bonding is significantly larger compared to the σ-bonding, in line with the theory that the strength of σ-donation is inversely correlated to the strength of π-acceptance. Still the phosphonite seems to be a weaker σ-donor compared to CO, reducing the π-basicity of the ruthenium and leading to a net upfield shift of the $^{31}P\{^1H\}$ NMR resonance in $[PAP(OEt_2)]_2Ru^{II}$(DPP) compared to $[PAP(OEt)_2]Ru^{II}$(CO)(DPP). Significantly, the relative line widths of the phosphorus resonances in the mono-complex (sharp) and in the bis-complex (broad) are reversed compared to the phosphines. Accordingly, the values of K_{a1} and K_{a2} are the largest, but K_{a3} displays the smallest value of the complexes. The first binding of $PAP(OEt)_2$, which leads to a more stable complex than with the phosphines but weakens the *trans*-CO considerably, has an overall negative effect on the second binding. The decrease of the K_{a3} by about 2 orders of magnitude compared to DPAP and DPPA is not reflected in the Ru−P bond length, which would be expected to be the longest (apart from PPh_3), and also contradicts the expectations based on the π-acceptor ability (judged from the IR shift) and on the cone angle θ.[25,46] Additionally, d(Ru−P) is not significantly decreased due to strong Ru→P π-back-bonding.[10]

To summarize the observations, the following series were obtained:

K_{a1}	$PPh_3 < (PA)_3P <$ DPAP, DPPA $< PAP(OEt)_2$
K_{a3}	$PAP(OEt)_2 < (PA)_3P <$ DPAP, DPPA
σ-donor strength	$(PA)_3P <$ DPAP $< PPh_3 < PAP(OEt)_2$
π-acceptor strength	$PPh_3<$ DPAP, DPPA $< (PA)_3P < PAP(OEt)_2$

Conclusions

We have investigated the effect of complexation of different phosphorus ligands on the stability, solid state structure, and spectroscopic properties of $(MeOH)Ru^{II}$(CO)-(DPP) **2**. The mono-phosphine complexes $(PR_3)Ru^{II}$(CO)-(DPP) are readily formed in solution in quantitative yields. Due to their kinetic lability and the weakening of the carbonyl ligand via a trans effect, the mono-phosphine complexes could not be isolated. The bis-phosphine complexes can be isolated in pure form by crystallization from $CHCl_3$−MeOH solutions using excess ligand. The X-ray structure solutions of the bis-phosphine complexes show only marginal differences in the geometrical parameters in the solid state.

(58) Xu, D. F.; Murfee, H. J.; van der Veer, W. E.; Hong, B. *J. Organomet. Chem.* **2000**, *596*, 53.
(59) Saenger, W. *Principles of Nucleic Acid Structure*; Springer-Verlag: New York, 1984.
(60) Darling, S.; Feeder, N.; Sanders, J. K. M. 1999, private communication to the CCDC.
(61) Stulz, E.; Sanders, J. K. M.; Montalti, M.; Prodi, L.; Zaccheroni, N.; Fabrizi de Biani, F.; Grigiotti, E.; Zanello, P. *Inorg. Chem.* **2002**, *41*, 5269.
(62) This structure has been communicated previously to the CCDC (CSD refcode: HOJBAJ) but is described here in detail for the first time.[60]
(63) Originally, we had also included the primary phosphine PhC≡C−PH_2 in our series. However, this ligand has proven to be very reactive toward protic solvents and unstable with respect to oxidation, and therefore unsuitable for the studies presented here; detailed studies will be presented elsewhere. The $^{31}P\{^1H\}$ NMR chemical shifts were included into the correlation to the pK_a to improve the range of the regression. $pK_a = -3.69$;[53] $\delta(^{31}P)$: −180 ppm (free ligand), −121 ppm (mono-phosphine complex).
(64) Diagnostic NMR shifts were obtained from the ^{31}P nucleus, but theoretically the chemical shift differences upon complexation cannot be assigned purely to electronic effects upon formation of the Ru−P bond, because the influence of the ring current of the aromatic porphyrin system also has to be taken into account. The binding site of a ligand to a metalloporphyrin is located in the strongly shielding region of the π-system of the porphyrin, leading to a significant upfield shift of the resonance of the respective nuclei. As judged from proton NMR spectroscopy, however, the solution state geometries of the complexes are almost identical in all cases. The relative positions of the phosphorus atoms vary by 0.06 Å along the Ru−P axis orthogonal to the porphyrin plane. We assume the influence of the bond length differences to be negligible, and the observed chemical shift differences to arise from the electronic effects of the different bond types and a constant upfield shift caused by the ring current of the aromatic ring system. This problem has not been addressed as such in previous studies.

The cone angle results demonstrate that mathematically derived steric ligand parameters alone do not necessarily represent an accurate model to predict solution stability of phosphorus complexes. Also, it is not clear why an acetylenic spacer, which introduces a structural gap between the phosphorus and the phenyl ring when the phosphine is put into an energetically minimized propeller twist conformation, should not alter the steric demand of the ligand. But in our system the K_a values span a range of 2 orders of magnitude, which may be too small to detect a significant effect arising purely from θ. Other comparisons of θ with stability constants utilize systems where the association constants vary by more than 5 orders of magnitude.[22]

The association constant K_{a1} for PPh_3 to $(MeOH)Ru^{II}(CO)$-(DPP) is the smallest value measured, which is not in line with the pK_a, $\delta(^{31}P)$, or θ values. Replacement of one phenyl substituent for an alkynylphenyl substituent on the phosphine has a large influence on the overall binding, and the thermodynamic stability increases by a factor of ~100. On the other hand, if all phenyl groups are replaced, the K_{a1} value drops back by a factor of 10, attributed to electronic factors. It is also noteworthy that DPAP and DPPA seem to have very similar stereoelectronic properties despite the attachment of an additional phosphorus at the acetylene substituent. The K_{a2} values show that the first binding of the ligands is decreased 4-fold upon decarbonylation, which can be attributed to a trans effect of the CO ligand.[18] Association to form the complexes $(PR_3)_2Ru^{II}(DPP)$ for the phosphines is in a range similar to that for the first binding to $(MeOH)Ru^{II}(CO)(DPP)$, but for the phosphonite PAP-$(OEt)_2$, binding is decreased 100-fold.

In summary, there is no simple correlation between the individual spectroscopic values, the electronic and steric effects, and the thermodynamic stability. The separation of the electronic effects into pure σ-donor and π-acceptor properties is generally oversimplified, and the overall electronic density on the phosphorus has to be taken into account. It remains to be evaluated whether the data can be used to improve further the attempted calculations (ECW or QALE model) on the stereoelectronic factors influencing the properties of phosphines. We propose, however, that $^{31}P\{^1H\}$ NMR spectroscopy can be used to estimate the pK_a, and probably other stereoelectronic parameters, of a phosphorus ligand when $\Delta\delta(^{31}P)$ is determined for $(PR_3)Ru^{II}(CO)$-(DPP). The influence of the different ligands on the photophysical and electrochemical behavior of Ru^{II}(DPP) will be discussed in the following paper.[61]

Acknowledgment. The diffraction data of $[PAP(OEt_2)]_2$-Ru^{II}(DPP) were collected by John E. Davies, Cambridge. Financial support from the Swiss National Science Foundation (Grant 8220-061293 to E.S.) and from the EPSRC is gratefully acknowledged. We thank Amy L. Kieran for careful revision of the manuscript. Helpful comments of referees are gratefully acknowledged.

Supporting Information Available: X-ray crystallographic tables for structures **12**, **13**, **14**, and **15** (atomic coordinates, bonds lengths and angles, anisotropic thermal factors, hydrogen atom positions as CIFs); nonlinear least-squares fitting data for the UV−vis titrations of **2** with **3**, **5**, **6**, and **7**; Gaussian deconvolution data for the UV−vis dilution series of **12**, **13**, **14**, and **15**. This material is available free of charge via the Internet at http://pubs.acs.org.

IC025727Y